

Kirby diagrams, trisections and gems of PL 4-manifolds: relationships, results and open problems

MARIA RITA CASALI¹ AND PAOLA CRISTOFORI²

^{1,2}*Department of Physics, Informatics and Mathematics, University of Modena and Reggio Emilia
Via Campi 213 B, I-41125 Modena (Italy), casali@unimore.it, paola.cristofori@unimore.it*

February 5, 2025

Abstract

We review the main achievements regarding the interactions between gem theory (which makes use of edge-colored graphs to represent PL-manifolds of arbitrary dimension) and both the classical representation of PL 4-manifolds via Kirby diagrams and the more recent one via trisections. Original results also appear (in particular, about gems representing closed 4-manifolds which need 3-handles in their handle decomposition, as well as about trisection diagrams), together with open problems and further possible applications to the study of compact PL 4-manifolds.

Keywords: trisection, Kirby diagram, edge-colored graph

2020 Mathematics Subject Classification: 57Q15 - 57K40 - 57M15

1 Introduction

Gem theory is a well-established representation theory for PL-manifolds of arbitrary dimension, whose combinatorial tool are edge-colored graphs, dual to colored triangulations (see, for example, [9] and references therein). In dimension four, it has been proved to have interesting interactions both with the classical representation via Kirby diagrams (or, equivalently, handle decompositions) and with the more recent one via trisections. In particular, algorithmic procedures have been obtained, to pass from one representation to the other (see [8], [10] and [11]), allowing to yield estimations of the involved invariants and to produce examples of triangulations of exotic 4-manifolds in order to investigate their PL structures.

The present paper reviews the main achievements on the subject, together with open problems and further possible applications to the study of compact PL 4-manifolds. In order to help the reader gain a deep understanding of the above interactions, without forcing him to continually refer to previous papers, sketches of the main proofs are provided, so as to make the text essentially self-contained.

Original results also appear, which improve the state-of-the-art and open to further developments. In particular, some typical situations are identified, for which it is possible to obtain a gem of a closed 4-manifold described by a handle decomposition, starting from a gem of the compact 4-manifold consisting only of the handles up to order two: see Proposition 9 and related examples. Moreover, in Section 3.3.1, we explain how to obtain trisection diagrams directly from gems admitting gem-induced trisections and/or from Kirby diagrams, via gem theory.

The paper is organized as follows.

Section 2 is devoted to a brief review of the basic notions about the three involved representation methods for PL 4-manifolds, i.e. Kirby diagrams, trisections and colored graphs. Section 3 contains

the main results and constructions about the relationships among the three theories: in particular, from Kirby diagrams to gems (Section 3.1, which contains also the original result related to the addition of 3-handles), from gems to trisections (Section 3.2) and from Kirby diagrams to trisections via gems (Section 3.3). Within the latter, the original part regarding trisection diagrams is presented, showing how trisection diagrams can be easily obtained from gems of 4-manifolds admitting gem-induced trisections (Proposition 21), and in particular from gems associated to Kirby diagrams (Proposition 22); by a suitable extension of the notion of trisection diagram, similar results are also obtained for simply-connected compact 4-manifolds with connected boundary (Proposition 23), in particular starting from their Kirby diagrams (Proposition 24). All these results closely resemble the already known ones in dimension 3, where gems of 3-manifolds, both in the closed and boundary case, directly yield Heegaard diagrams.

Finally, Section 4 completes the paper with a list of open problems, suggesting trends for future investigation.

2 Preliminaries about the involved representations

In this Section we briefly review the basic notions of the three representation methods for PL 4-manifolds involved in the paper, without any claim to exhaustiveness. Throughout the paper all manifolds and maps, when not specified, are understood to be PL. For generalities about 4-dimensional topology of piecewise linear manifolds, we refer to [27] and [23].

In the following, \mathbb{Y}_m will denote the orientable 4-dimensional handlebody of genus m , i.e. $\natural_m(\mathbb{S}^1 \times \mathbb{D}^3)$, while $\mathbb{Y}_m^{(\sim)}$ (resp. $\mathbb{S}^1 \otimes \mathbb{S}^{n-1}$) will denote a genus g 4-dimensional handlebody (resp. an \mathbb{S}^{n-1} -bundle over \mathbb{S}^1), orientable or non-orientable according to the context.

Obviously $\partial\mathbb{Y}_m^{(\sim)} = \#_m(\mathbb{S}^1 \otimes \mathbb{S}^2)$ and, whenever orientability is assumed, the n -sphere (resp. the 4-disk) will be included in the notation $\#_m(\mathbb{S}^1 \otimes \mathbb{S}^{n-1}) = \#_m(\mathbb{S}^1 \times \mathbb{S}^{n-1})$ (resp. $\mathbb{Y}_m^{(\sim)} = \mathbb{Y}_m$) as the case $m = 0$.

2.1 Kirby diagrams of orientable 4-manifolds

It is well-known that, if a compact orientable 4-manifold M admits a handle decomposition with no 3-handles, then M can be represented by a *Kirby diagram*, i.e. a link in the 3-sphere equipped with some further information, which encodes the attachments of 1- and 2-handles.

In fact, since the existence of exactly one 0-handle can always be assumed, then 1- and 2-handles can be visualized, by positioning on the boundary of the 0-handle, as follows:

- the attachment of each 2-handle is represented by a *knot* (i.e. the core of its attaching solid torus) equipped with an integer specifying the *framing* of the handle (i.e. the choice of a normal vector field on the knot);
- the attachment of a 1-handle would be specified by its attaching region formed by two 3-balls. However, this representation involves some technical issues, which lead to often prefer the so-called *Akbulut's notation*: this is based on the observation that the attachment of a 1-handle can be also thought of as the drilling of its complementary 2-handle. Therefore, each 1-handle can be visualized by drawing the boundary of the cocore of its complementary 2-handle, which is an unknot with no framing, and it is marked by a dot to distinguish it from the components that come from “real” 2-handles ([23]).

The resulting object is therefore a link L in the 3-sphere having some *framed* components equipped with integers and some *dotted* ones. Furthermore, it is always possible to arrange the handles in such a way that the dotted components, if any, are pairwise unlinked.

Obviously M can be re-constructed from \mathbb{D}^4 by adding 1-handles according to the dotted and 2-handles according to the framed components of L ; furthermore, ∂M is the closed 3-manifold obtained

by Dehn surgery on the framed link obtained by replacing each dotted component of L by a 0-framed one ([23] and [27]).

In particular, if $\partial M \cong \#_r(\mathbb{S}^1 \times \mathbb{S}^2)$ ($r \geq 0$), a famous result of Laudenbach and Poenaru ([25]) ensures that there is a unique way to attach r 3-handles and a 4-handle to obtain a closed manifold \bar{M} , which is then uniquely associated with M . As a consequence, in this case, any Kirby diagram representing M can be thought of as representing $\bar{M} = M \cup \mathbb{Y}_r$ as well.

In [32], Kirby diagrams representing closed orientable 4-manifolds (i.e. representing compact 4-manifolds with boundary homeomorphic to $\#_r(\mathbb{S}^1 \times \mathbb{S}^2)$, with $r \geq 0$) are also called (*4-dimensional Heegaard diagrams*).

2.2 Trisections of closed 4-manifolds

By generalizing the classical idea of Heegaard splitting in dimension 3, in 2016 Gay and Kirby ([22]) introduced the notion of *trisection* of a smooth closed oriented 4-manifold; then, the notion was extended to non-orientable 4-manifolds in [34] and [31].

Theorem 1 ([22], [34], [31]) *Each smooth closed orientable (resp. non-orientable) 4-manifold M admits a decomposition $M = H_0 \cup H_1 \cup H_2$, such that:*

- (a) H_0, H_1, H_2 are 4-dimensional orientable (resp. non-orientable) handlebodies with pairwise disjoint interiors;
- (b) $H_{01} = H_0 \cap H_1$, $H_{02} = H_0 \cap H_2$ and $H_{12} = H_1 \cap H_2$ are 3-dimensional orientable (resp. non-orientable) handlebodies with the same genus;
- (c) $\Sigma = H_0 \cap H_1 \cap H_2$ is a closed connected orientable (resp. non-orientable) surface.

Definition 1 ([22], [34], [31]) A triple (H_0, H_1, H_2) that satisfies the requirements of Theorem 1 is said to be a *trisection* of M ; the *genus* of such a trisection is defined as the common genus of the 3-dimensional handlebodies H_{01}, H_{02}, H_{12} , while the surface Σ is called the *central surface* of the trisection.¹

The *trisection genus* of a smooth closed 4-manifold M is defined as the minimum genus of a trisection of M .

It is not difficult to check that, if (H_0, H_1, H_2) is a genus g trisection of M , then (Σ, H_{ij}, H_{ik}) is a genus g Heegaard splitting of ∂H_i , for each permutation (i, j, k) of $\{0, 1, 2\}$. Moreover, if k_i ($i \in \{0, 1, 2\}$) denotes the genus of the 4-dimensional “piece” H_i , the equality $\chi(M) = 2 + g - k_0 - k_1 - k_2$ holds, together with the inequalities $g \geq \beta_1(M; \mathbb{Z}_2) + \beta_2(M; \mathbb{Z}_2)$ and $\beta_1(M; \mathbb{Z}_2) \leq k_i, \forall i \in \{0, 1, 2\}$.

As a consequence, only simply-connected 4-manifolds can admit trisections where one the 4-dimensional “pieces” is a 4-disk. Viceversa, it is an open problem whether each closed simply-connected 4-manifold admits a trisection with this property, or not: see, for example, [29], [24] and [30].

In virtue of the already cited theorem by Laudenbach and Poenaru ([25]), together with its non-orientable version proved in [31], the attachments of the 3-dimensional handlebodies on the central surface are sufficient to identify the trisection, and hence the represented closed 4-manifold:

¹Note that in the orientable (resp. non-orientable) case the genus of the central surface equals (resp. is the double of) the genus of the trisection. Actually, many slightly different versions of the notions regarding trisections exist, also in the cited papers, for example requiring that all 4-dimensional handlebodies have the same genus (giving rise to the so-called *balanced trisections*), or considering the genus of the central surface as the genus of the trisection, also in the non-orientable case. However, no loss of generality occurs, and it is not difficult to translate one version into the others.

Definition 2 A $(g; k_0; k_1; k_2)$ -trisection diagram is a 4-tuple $(\Sigma; \alpha, \beta, \gamma)$ such that the triples $(\Sigma; \alpha, \beta)$, $(\Sigma; \alpha, \gamma)$ and $(\Sigma; \beta, \gamma)$ are genus g Heegaard diagrams for $\#_{k_0}(\mathbb{S}^1 \otimes \mathbb{S}^2)$, $\#_{k_1}(\mathbb{S}^1 \otimes \mathbb{S}^2)$ and $\#_{k_2}(\mathbb{S}^1 \otimes \mathbb{S}^2)$ respectively.²

In fact - as explained in [31] both in the orientable and non-orientable setting - the 4-manifold M is uniquely obtained, up to diffeomorphism, in the following way:

- take the product $\Sigma \times \mathbb{D}^2$;
- take three genus g 3-dimensional handlebodies V_α, V_β and V_γ , identified by the systems of curves α, β and γ respectively;
- attach $V_\alpha \times I$ (resp. $V_\beta \times I$) (resp. $V_\gamma \times I$) to $\partial(\Sigma \times \mathbb{D}^2) = \Sigma \times \mathbb{S}^1$ along $\Sigma \times [-\epsilon, \epsilon]$ (resp. $\Sigma \times [\frac{2}{3}\pi - \epsilon, \frac{2}{3}\pi + \epsilon]$) (resp. $\Sigma \times [\frac{4}{3}\pi - \epsilon, \frac{4}{3}\pi + \epsilon]$);
- fill the three boundary components (isomorphic to $\#_{k_i}(\mathbb{S}^1 \otimes \mathbb{S}^2)$, for $i = 0, 1, 2$) of the resulting compact 4-manifold with three 4-dimensional handlebodies (of genus k_i , for $i = 0, 1, 2$).

2.3 Gems

Crystallization theory, or *gem theory* is a representation tool for piecewise linear (PL) compact manifolds, without assumptions about dimension, connectedness, orientability or boundary properties. For a detailed review of the foundational notions and results, see the “classical” survey paper [20], or the book [26] regarding dimension 3; for updated developments, especially in dimension 4, see [9] and [13], together with their references. Here, we summarize only the basic elements that are necessary for the topic we are interested in.

Definition 3 An $(n+1)$ -colored graph ($n \geq 2$) is a pair (Γ, γ) , where $\Gamma = (V(\Gamma), E(\Gamma))$ is a multigraph (i.e. multiple edges are allowed, while loops are forbidden) which is regular of degree $n + 1$, and γ is an *edge-coloration*, that is a map $\gamma : E(\Gamma) \rightarrow \Delta_n = \{0, \dots, n\}$ which is injective on adjacent edges.

For sake of concision, the coloration γ is often understood, and the colored graph is simply denoted by Γ .

For every $\{c_1, \dots, c_h\} \subseteq \Delta_n$ let $\Gamma_{\{c_1, \dots, c_h\}}$ be the subgraph obtained from Γ by deleting all the edges that are not colored by the elements of $\{c_1, \dots, c_h\}$. In this setting, the complementary set of $\{c\}$ (resp. $\{c_1, \dots, c_h\}$) in Δ_n will be denoted by \hat{c} (resp. $\hat{c}_1 \cdots \hat{c}_h$). The connected components of $\Gamma_{\{c_1, \dots, c_h\}}$ are called $\{c_1, \dots, c_h\}$ -residues or h -residues of Γ ; their number is indicated by $g_{\{c_1, \dots, c_h\}}$ (or, for short, by $g_{c_1, c_2}, g_{c_1, c_2, c_3}$ and $g_{\hat{c}}$ if $h = 2, h = 3$ and $h = n$ respectively).

Within gem theory, an $(n + 1)$ -colored graph Γ is thought of as the combinatorial visualization of an n -dimensional pseudocomplex $K(\Gamma)$, which is associated to Γ in the following way:

- take an n -simplex for each vertex of Γ and label its vertices by the elements of Δ_n ;
- if two vertices of Γ are c -adjacent ($c \in \Delta_n$), glue the corresponding n -simplices along their $(n - 1)$ -dimensional faces opposite to the c -labelled vertices, so that equally labelled vertices are identified.

In general, $|K(\Gamma)|$ is an n -pseudomanifold and Γ is said to *represent* it.

By construction, $K(\Gamma)$ is endowed with a vertex-labeling by Δ_n that is injective on each simplex. Moreover, Γ turns out to be the 1-skeleton of the dual complex of $K(\Gamma)$. The duality establishes a bijection between the $\{c_1, \dots, c_h\}$ -residues of Γ and the $(n - h)$ -simplices of $K(\Gamma)$ whose vertices

²Obviously, all 3- and 4-dimensional manifolds involved in Definition 2, as well as in the procedure to reconstruct the represented closed 4-manifold, are orientable or not according to Σ .

are labelled by $\Delta_n - \{c_1, \dots, c_h\}$. In particular, given an $(n + 1)$ -colored graph Γ , each connected component of $\Gamma_{\hat{c}}$ ($c \in \Delta_n$) is an n -colored graph representing the link of a c -labelled vertex of $K(\Gamma)$ in the first barycentric subdivision of $K(\Gamma)$.

As a consequence, the following characterizations hold:

- $|K(\Gamma)|$ is a closed n -manifold iff, for each color $c \in \Delta_n$, all \hat{c} -residues of Γ represent the $(n - 1)$ -sphere;
- $|K(\Gamma)|$ is a singular³ n -manifold iff, for each color $c \in \Delta_n$, all \hat{c} -residues of Γ represent closed connected $(n - 1)$ -manifolds.

Remark 1 If N is a singular n -manifold, then a compact n -manifold \check{N} is easily obtained by deleting small open neighbourhoods of its singular vertices. Conversely, given a compact n -manifold M , a singular n -manifold \widehat{M} can be constructed by capping off each component of ∂M by a cone over it.

Throughout the paper, we will restrict to the class of compact 4-manifolds without spherical boundary components, where the above correspondence is bijective; hence, singular n -manifolds and compact n -manifolds can be associated each other in a well-defined way. Obviously, in this wider context, closed n -manifolds are characterized by $M = \widehat{M}$.

In virtue of the bijection described in Remark 1, an $(n + 1)$ -colored graph Γ is said to *represent* a compact n -manifold M (or, equivalently, to be a *gem* of M , where gem means *Graph Encoding Manifold*) if and only if it represents the associated singular manifold \widehat{M} .

A \hat{c} -residue of a gem Γ will be called *singular* if it corresponds to a singular vertex of $|K(\Gamma)|$, i.e. if it does not represent the sphere, while a color c is said to be *singular* if at least one \hat{c} -residue is singular.

Gem theory (or *crystallization theory*) is based on the following existence theorem, which extends to the boundary case the foundational one due to Pezzana for closed manifolds of arbitrary dimension (see [20]).

Theorem 2 ([14]) *Any compact n -manifold M admits a gem Γ , that is bipartite if and only if M is orientable.*

In particular, if M has empty or connected boundary:

- Γ may be assumed to have color n as its unique possible singular color, and exactly one \hat{n} -residue (in this case we will say that Γ belongs to the class $G_s^{(n)}$);
- Γ may be assumed to have exactly one \hat{c} -residue, $\forall c \in \Delta_n$ (in this case Γ is called a *crystallization of M*).

Within gem theory, a finite set of combinatorial moves have been defined, which translate the homeomorphism problem of the represented manifolds.

Definition 4 An r -dipole ($1 \leq r \leq n$) of colors c_1, \dots, c_r of an $(n + 1)$ -colored graph Γ is a subgraph consisting of two vertices, belonging to different connected components of $\Gamma_{\hat{c}_1 \dots \hat{c}_r}$, that are joined by r edges, colored by c_1, \dots, c_r .

The *elimination* of an r -dipole in Γ can be carried out by deleting the subgraph and welding the remaining hanging edges according to their colors; in this way another $(n + 1)$ -colored graph Γ' is obtained. The inverse operation is called the *addition* of the dipole to Γ' .

Proposition 3 *Let Γ be a gem of a compact n -manifold M with empty or connected boundary. If Γ' is obtained from Γ by eliminating an r dipole ($1 \leq r \leq n$), then Γ' is a gem of M , too.*

³A *singular (PL) n -manifold* is a closed connected n -dimensional polyhedron admitting a simplicial triangulation where the links of vertices are closed connected $(n - 1)$ -manifolds. Vertices whose links are not $(n - 1)$ -spheres are called *singular*. The notion extends also to polyhedra associated to colored graphs, provided that links of vertices are considered in the first barycentric subdivision of $K(\Gamma)$.

Moreover, other combinatorial moves have been defined, whose effects on the represented manifolds turn out to be significant also in the context of the present paper (see Proposition 9, which gives an original contribution to the study of these moves, applied to colored graphs representing compact manifolds with non-empty boundary).

Definition 5 A ρ_h -pair ($1 \leq h \leq n$) of color $i \in \Delta_n$ in an $(n+1)$ -colored graph Γ is a pair of i -colored edges (e, f) sharing the same $\{i, c\}$ -colored cycle for each $c \in \{c_1, \dots, c_h\} \subseteq \Delta_n$.

The *switching* of (e, f) consists in canceling e and f and establishing new i -colored edges between their endpoints; the reversed operation is obviously the switching of a ρ_{n-h} -pair. Although, in general, the switching can be performed in two different ways, it is uniquely determined if $\Gamma \in G_s^{(n)}$, $h \in \{n-1, n\}$ and the bipartition of each non-singular \hat{c} -residue is preserved.

The topological effects of the switching of ρ_{n-1} - and ρ_n -pairs have been completely determined in the case of closed n -manifolds: see [1], where it is proved that a ρ_{n-1} -pair (resp. ρ_n -pair) switching does not affect the represented n -manifold (resp. either induces the splitting into two connected summands, or the “loss” of a $\mathbb{S}^1 \otimes \mathbb{S}^{n-1}$ summand in the represented n -manifold).

Finally, we point out that an interesting aspect of gem theory is related to the possibility of combinatorially defining PL invariants of manifolds in arbitrary dimension. The most important one, which extends to higher dimension the classical genus of a surface and the Heegaard genus of a 3-manifold, is founded on the existence of a particular type of embedding of colored graphs into surfaces.

Proposition 4 ([20]) *Let Γ be a connected bipartite (resp. non-bipartite) $(n+1)$ -colored graph of order $2p$. Then for each cyclic permutation $\varepsilon = (\varepsilon_0, \dots, \varepsilon_n)$ of Δ_n , up to inverse, there exists a cellular embedding, called regular, of Γ into an orientable (resp. non-orientable) closed surface $F_\varepsilon(\Gamma)$ whose regions are bounded by the images of the $\{\varepsilon_j, \varepsilon_{j+1}\}$ -colored cycles, for each $j \in \mathbb{Z}_{n+1}$. Moreover, the genus (resp. half of the genus) of $F_\varepsilon(\Gamma)$, denoted by $\rho_\varepsilon(\Gamma)$, satisfies*

$$2 - 2\rho_\varepsilon(\Gamma) = \sum_{j \in \mathbb{Z}_{n+1}} g_{\varepsilon_j, \varepsilon_{j+1}} + (1 - n)p.$$

Throughout the paper, for sake of notational simplicity, if $i \in \Delta_n$ is such that $g_i = 1$, we will write $\rho_\varepsilon(\Gamma_{\hat{i}})$ (resp. $F_\varepsilon(\Gamma_{\hat{i}})$) instead of $\rho_{\varepsilon'}(\Gamma_{\hat{i}})$ (resp. $F_{\varepsilon'}(\Gamma_{\hat{i}})$), ε' being the permutation induced by ε on \hat{i} .

Definition 6 The *regular genus* of an $(n+1)$ -colored graph Γ is defined as

$$\rho(\Gamma) = \min\{\rho_\varepsilon(\Gamma) \mid \varepsilon \text{ cyclic permutation of } \Delta_n\},$$

while the *regular genus* of a compact n -manifold M is defined as

$$\mathcal{G}(M) = \min\{\rho(\Gamma) \mid \Gamma \text{ gem of } M\}.$$

Since the number of vertices of a gem, i.e. the number of n -simplices in the dual triangulation, can be interpreted as a measure of the “complexity” of the represented manifold, another PL invariant naturally arises:

Definition 7 For each compact n -manifold M , its *gem-complexity* is the non-negative integer $k(M) = p - 1$, where $2p$ is the minimum order of an $(n+1)$ -colored graph representing M .

Remark 2 Many significant classification results have been obtained within crystallization theory, with respect to both regular genus and gem-complexity: see, for example, [16] for a review regarding dimension 4. Regular genus and gem-complexity are also proved to be related to the *G-degree*, a PL invariant arising within the theory of *Colored tensor models* in theoretical physics: this relation is investigated - among other - in [15] and [14]. The topic of the present paper highlights further connections of the above invariants with those based on other representation tools for PL 4-manifolds.

3 Relationships and results

3.1 From Kirby diagrams to gems

In this section we will describe an algorithm to obtain a gem $\Gamma(L, d)$ of a compact (orientable) 4-manifold M starting from a Kirby diagram (L, d) of M , where L is a link in \mathbb{S}^3 and d a vector that contains the framings. More precisely, we suppose that L has l components, L_1, \dots, L_l , whose first m , if any, are dotted and, for each $i \in \{1, \dots, l - m\}$, d_i is the framing of $(m + i)$ -th component.

Actually, the construction is performed on a planar diagram of L , which we suppose fixed and, for sake of simplicity, will also be called L ; hence we will refer to all combinatorial characteristics of the diagram (such as *arcs*, *crossings* and *regions*) as of L itself. Moreover, we assume that the diagram is connected⁴ and *self-framed*, i.e. the writhe of each non-dotted component equals its framing. Note that this last requirement can be always satisfied up to the addition of positive or negative curls.

The starting step of the procedure is the construction of a 4-colored graph $\Lambda(L, d)$ representing the 3-manifold ∂M , which, as recalled in Section 2.1, is obtained by Dehn surgery on \mathbb{S}^3 along the framed link associated to L . As it is easily seen from the example in Figure 3, $\Lambda(L, d)$ can be directly “drawn over” L , by taking the subgraph of order eight depicted in Figure 1 for each crossing, while to each curl there corresponds a subgraph of one of the two types in Figure 2 according to the curl being positive or negative.

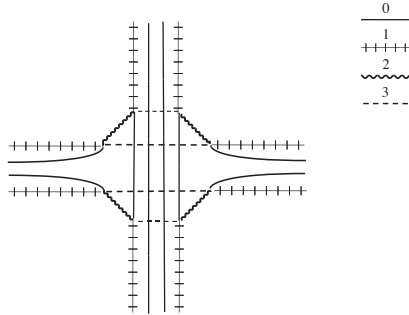


Figure 1: subgraph corresponding to a crossing



Figure 2: subgraphs corresponding to a positive (left) or negative (right) curl

A central role is played in the algorithm by a combinatorial structure, called a *quadrilateral*, consisting of four vertices $\{P_0, P_1, P_2, P_3\}$ such that, for each $i \in \mathbb{Z}_4$, P_i and P_{i+1} are i -adjacent and P_i does not belong to the $\{i + 1, i + 2\}$ -colored cycle shared by the other three vertices. We point out that a quadrilateral always arises between the subgraphs corresponding to a curl and an undercrossing or between two curls; therefore, up to the addition of a pair of opposite curls, the existence of a quadrilateral can always be assumed on each framed component of L .

In the special case of $m = 0$, i.e. when dotted components are missing, the procedure to obtain a gem $\Gamma(L, d)$ of M is particularly simple: it is sufficient to double by 4-colored edges all 1-colored edges of $\Lambda(L, d)$ except among the vertices of a quadrilateral for each (framed) component, where the addition of 4-colored edges is done as shown in Figure 4 (see also Figure 5 for an example where (L, d) is a trefoil with framing $+1$).

⁴We point out that any Kirby diagram can be made so by suitable Reidemeister moves. Alternatively, the algorithm can be applied to each connected component and then graph-connected sums can be performed on the resulting gems in order to obtain a 5-colored graph representing M (see [11] for details).

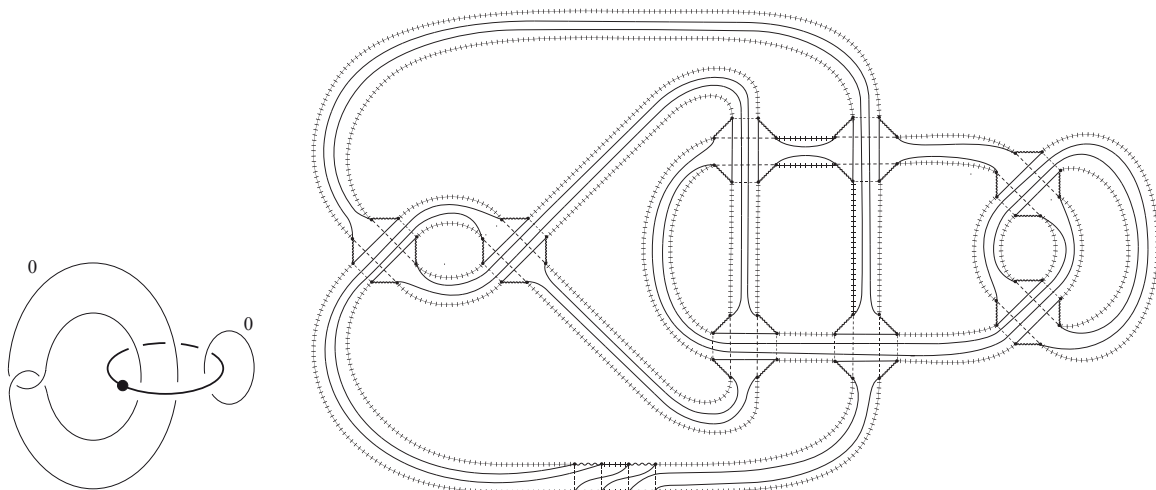


Figure 3: A Kirby diagram of $S^2 \times \mathbb{D}^2$ and a gem of its boundary

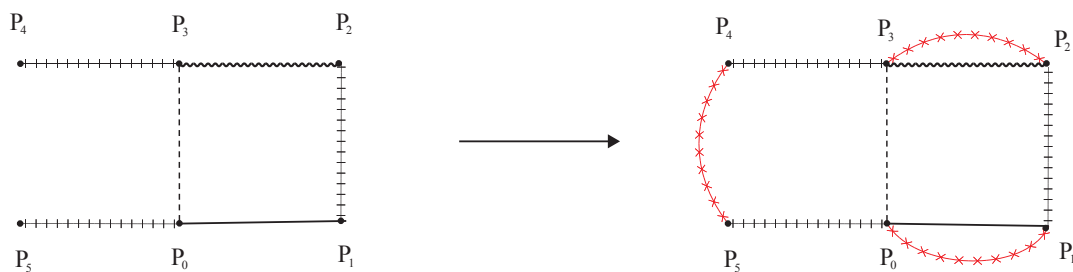


Figure 4: The attachment of 4-colored edges among the vertices of a quadricolor

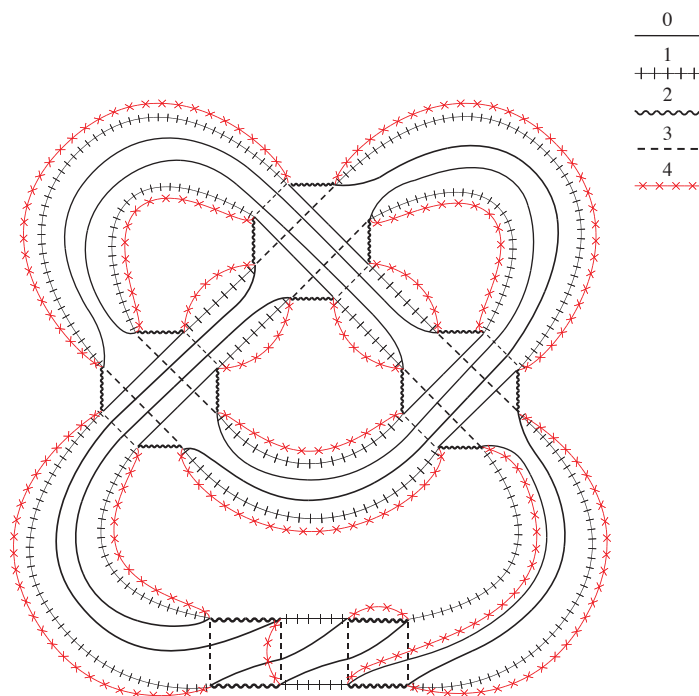


Figure 5: The 5-colored graph $\Gamma(L, d)$ obtained from the framed link $(K_T, +1)$, K_T being the trefoil knot

The case when dotted components appear requires some further hypotheses and some choices of points and parts of arcs of the diagram, each choice producing at the end a different graph but all

representing the compact manifold encoded by the Kirby diagram.

The dotted components are assumed to be in *good position*, i.e. they are unknotted, unlinked and on each of them overcrossings and undercrossings never alternate⁵.

The choices we are listing below will determine how to add the 4-colored edges to the gem $\Lambda(L, d)$ of ∂M which has been previously constructed:

- on each dotted component L_i ($i \in \{1, \dots, m\}$) two points H_i and H'_i must be “marked”, such that they divide it into two parts, one containing only overcrossings and the other containing only undercrossings;
- for each $i \in \{m + 1, \dots, l\}$ the framed component L_i is “cut” in a point X_i between a curl and an undercrossing or between two curls; moreover, starting from X_i in the direction opposite to the undercrossing (or in any direction if X_i lies between two curls) let’s “highlight” a sequence of consecutive segments of arcs of $L_i \setminus X_i$, so that for each dotted component L_j the points H_j and H'_j belong to the boundary of the same region \mathcal{R}_j of the plane determined by L with all cuts and highlighted segments removed.

Figure 6 shows an example of choices where the determined region, \mathcal{R}_1 , is the union of the gray ones with the unbounded region. Figure 7 shows examples of different choices on the same Kirby diagram.

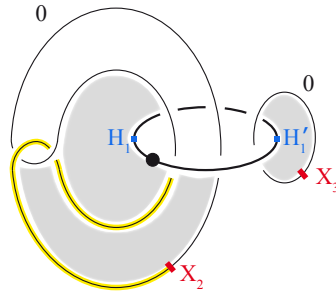


Figure 6:

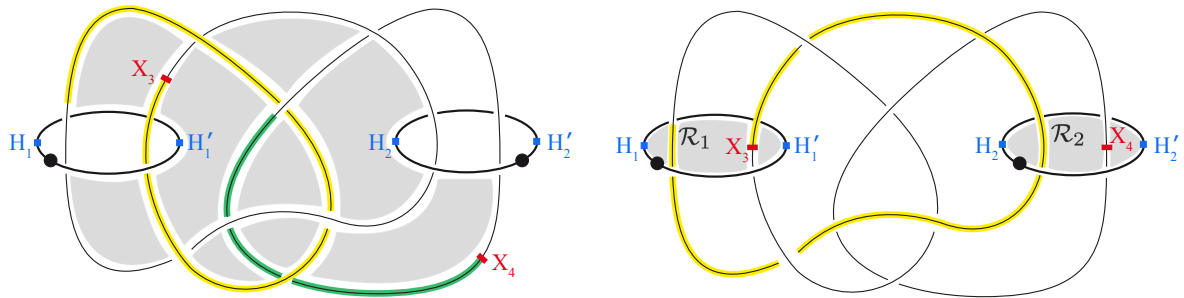


Figure 7: Different choices on the same diagram: $\mathcal{R}_1 = \mathcal{R}_2$ on the left; $\mathcal{R}_1 \neq \mathcal{R}_2$ and an empty sequence of highlighted segments for L_4 on the right

The above choices allow to determine the attachments of the 4-colored edges to $\Lambda(L, d)$ in order to obtain $\Gamma(L, d)$ as follows:

- for each $i \in \{m + 1, \dots, l\}$, a quadricolor can be detected in $\Lambda(L, d)$ in correspondence with the cut X_i and so the triple of 4-colored edges among its vertices is added according to Figure 4;

⁵This assumption does not involve any loss of generality since, by suitably arranging handles and possibly using Reidemeister moves, any compact orientable 4-manifold turns out to admit a Kirby diagram whose dotted components are in good position.

- for each quadricolor, starting from the two vertices 1-adjacent to P_4 and P_5 (see Figure 4), 4-colored edges are added, following the sequence of highlighted segments of arcs and respecting bipartition classes, among the vertices of each pair of 1-colored edges which are “parallel” to a highlighted segment;
- the 0-colored edges corresponding to any undercrossing which is “met” by the sequence are doubled by 4-colored edges;
- for each $i \in \{1, \dots, m\}$ the points H_i and H'_i allow to identify, on the subgraph corresponding to the dotted component L_i , two pairs of vertices (v_i, w_i) and (v'_i, w'_i) , which are the endpoints of the two 1-colored edges separating overcrossings from undercrossings and lie on the side of the region \mathcal{R}_i ; then a 4-colored edge is added between v_i and v'_i and between w_i and w'_i ;
- the missing 4-colored edges are added so as to obtain a cycle from each $\{1, 4\}$ -colored path.

Figure 8 shows the application of the above algorithm to the example of Figure 6.

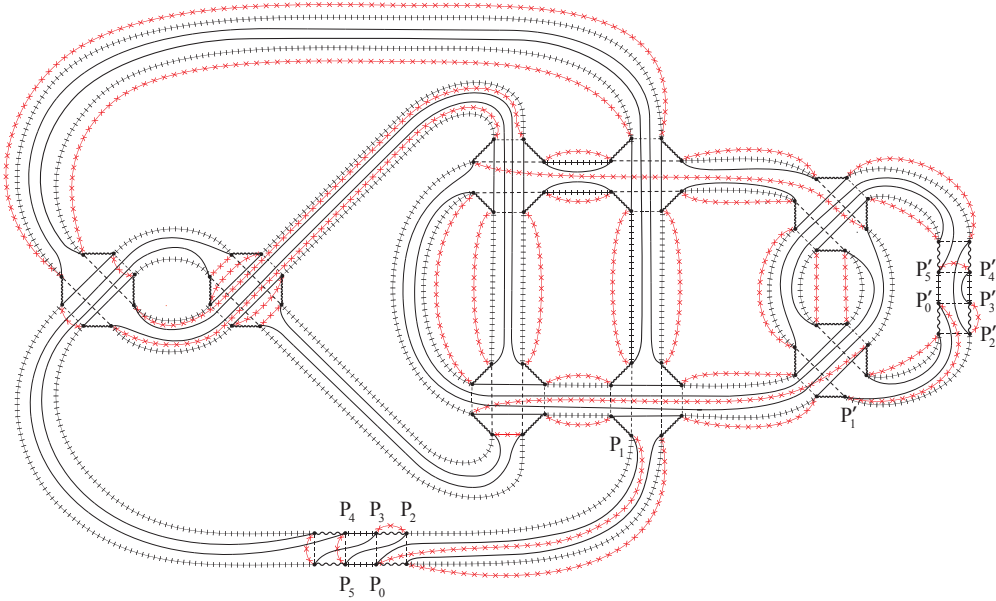


Figure 8:

Theorem 5 ([8]) *Given a compact 4-manifold M , let (L, d) be a connected Kirby diagram representing it, where all dotted components, if any, are in good position. Then, the 5-colored graph $\Gamma(L, d)$ is a gem of M .*

The proof of the above result consists in showing that $\Gamma(L, d)$ can also be obtained from $\Lambda(L, d)$ by a sequence of combinatorial moves with a precise topological meaning. One of the most important is the so-called *smoothing of a quadricolor* which is the exchange of three 1-colored edges among the vertices of the quadricolor as depicted in Figure 9.

This move, done on a quadricolor of $\Lambda(L, d)$ corresponding to a given framed component L_i , produces a new 3-colored graph representing the 3-manifold obtained by Dehn surgery on the link obtained from L by adding the complementary knot of L_i (i.e. a 0-framed trivial knot linking the component L_i geometrically once), that is, essentially, by cancelling that framed component⁶.

⁶Quadricolors in 4-colored graphs were originally introduced by Lins ([26]). The smoothing of a quadricolor in a gem of a closed 3-manifold can also be interpreted as the substitution, in the dual triangulation, of a solid torus with another solid torus having the same boundary. Hence, it is equivalent to performing a Dehn surgery. In the specific case of $\Lambda(L, d)$, this surgery can be identified as the one along the complementary knot of the component naturally associated with the quadricolor (see [8, Proposition 9(i)] for details).

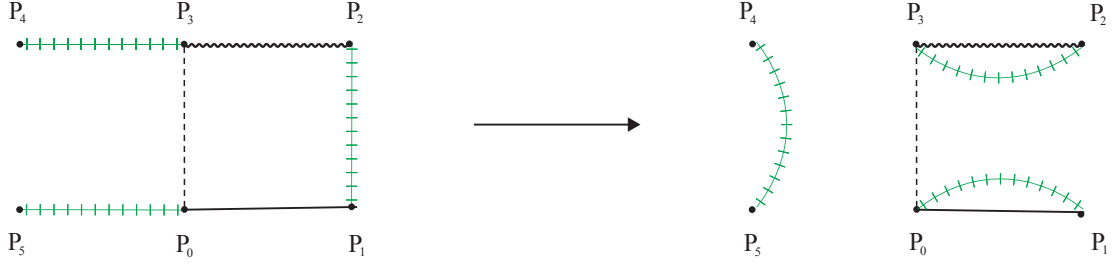


Figure 9: the smoothing of a quadricolor

Sketch of the proof (of Theorem 5):

First, let us note that, as visualized in Figure 11, the handle-decomposition encoded by (L, d) can be realized by considering a collar of $\#_m(\mathbb{S}^1 \times \mathbb{S}^2)$, where $m \geq 0$ is the number of dotted components of (L, d) , and attaching the 0- and 1-handles on one of its boundary component, the 2-handles on the other one. This can be done via gems in the following way.

- Starting from $\Lambda(L, d)$, let us perform the smoothing of all quadricolors of the framed components of (L, d) ; by what we have just observed, the result is a 4-colored graph $\tilde{\Lambda}$ representing $\#_m(\mathbb{S}^1 \times \mathbb{S}^2)$. By doubling the 1-colored edges of $\tilde{\Lambda}$ by 4-colored ones, a 5-colored graph $\tilde{\Gamma}$ is obtained which can be easily seen to represent $\#_m(\mathbb{S}^1 \times \mathbb{S}^2) \times I$, whose two boundary components are represented by the 4-colored graphs $\tilde{\Gamma}_1$ and $\tilde{\Gamma}_4$ respectively (see the central part of Figure 11).
- A sequence of ρ_2 -pairs of color 4 (see Section 2.3) can be detected in $\tilde{\Gamma}$, whose switchings are proved to preserve the represented manifold (topologically each switching simply produces a re-triangulation of the manifold).
- As a consequence of the ρ_2 -pairs switchings, in each subgraph corresponding to a dotted component L_i ($i \in \{1, \dots, m\}$) a ρ_3 -pair of color 4 appears, whose endpoints are exactly (v_i, w_i) and (v'_i, w'_i) . As pointed out in [8, Proposition 11], the switching of these ρ_3 -pairs, realized by connecting v_i with v'_i and w_i with w'_i by 4-colored edges for each $i \in \{1, \dots, m\}$, has the topological effect of an identification between the boundary of a genus m 4-dimensional handlebody (that is the union of 0- and 1-handles in the handle-decomposition encoded by (L, d)) and the component of the boundary of $\#_m(\mathbb{S}^1 \times \mathbb{S}^2) \times I$ represented by $\tilde{\Gamma}_1$ (the “red” boundary in Figure 11) after the ρ_2 -pairs switchings.
- Note that $\tilde{\Gamma}_4$, the “blue” boundary in Figure 11, has not been affected by the performed switchings of ρ_2 - and ρ_3 -pairs and, therefore, can be thought of as representing the boundary of the resulting 4-manifold (which is obviously homeomorphic to a genus m 4-dimensional handlebody).

In order to obtain $\Gamma(L, d)$, it is now sufficient to re-place the triples of 1-colored edges of the quadricolors in their original position (see Figure 10). As proved in [8, Proposition 9(ii)], for each framed component L_i ($i \in \{m+1, \dots, l\}$), this move on the associated quadricolor realizes the attachment of a 2-handle along L_i on the boundary component represented by $\tilde{\Gamma}_4$.

□

As a direct consequence of the construction, the order of $\Gamma(L, d)$ and its regular genus can be expressed in terms of the combinatorial properties of the Kirby diagram. Therefore, upper bounds for the value of the gem-complexity and the regular genus of the represented compact 4-manifold can be obtained:

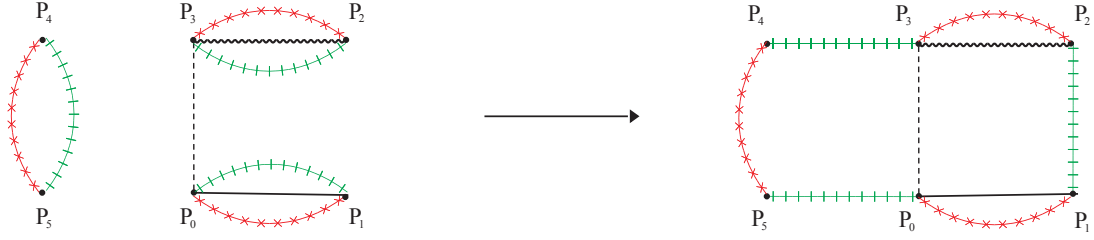


Figure 10: the attachment of a 2-handle

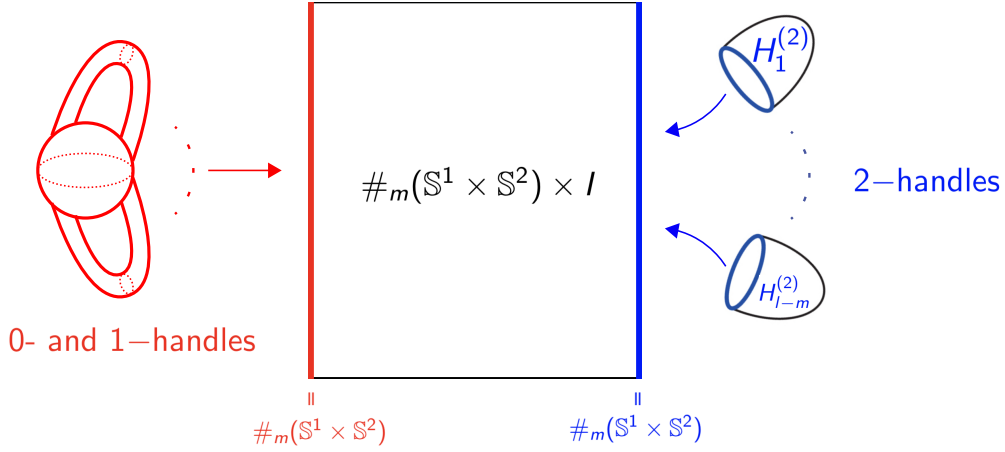


Figure 11: Realizing the handle-decomposition encoded by a Kirby diagram via gems (see proof of Theorem 5)

Theorem 6 ([8]) *Let M be a compact 4-manifold and let (L, d) be a connected Kirby diagram representing M , with l components whose dotted ones, if any, are in good position. Then:*

$$\mathcal{G}(M) \leq s + \bar{s} + (l - m) + 1$$

where $m \geq 0$ is the number of dotted components, s the number of crossings of (L, d) and \bar{s} the number of undercrossings of its framed components. Moreover, if L is different from the trivial knot:

$$k(M) \leq 2s + 2\bar{s} + 2m - 1 + 2 \sum_{i=1}^{l-m} t_i$$

where $t_i = 2$ if the writhe and the framing of the i -th framed component coincide, otherwise t_i is the absolute value of their difference.

We want to point out that, as proved in [6], if (L, d) has no dotted components, the 4-colored graph $\Lambda(L, d)$ contains some particular combinatorial configurations, called *generalized dipoles* that can be manipulated, thus obtaining a new 4-colored graph $\Omega(L, d)$, without changing the represented 3-manifold or affecting the quadricolors; by doubling by 4-colored edges the 1-colored ones and performing the moves on quadricolors of $\Omega(L, d)$ (i.e. by applying the construction to $\Omega(L, d)$ instead of $\Lambda(L, d)$), a 5-colored graph $\tilde{\Omega}(L, d)$ is obtained, still representing M , whose combinatorial structure allows to establish the following improvement of the estimation of the regular genus:

Theorem 7 ([8]) *Let M be a compact 4-manifold and let (L, d) be a connected Kirby diagram with no dotted components representing M . Then:*

$$\mathcal{G}(M) \leq m_\alpha + l$$

where l is the number of components of L and m_α is the number of α -colored regions in a chess-board coloration of L , α being the color of the unbounded region.

The following result - which can be easily proved by means of the above constructions (for details, see the proofs of [6, Theorem 1], [8, Theorem 7] or [10, Theorem 3]) - will turn out to be useful in Section 3.3.

Proposition 8 *Let (L, d) be a connected Kirby diagram, with s crossings, whose dotted components, if any, are in good position. If the cyclic permutation $\varepsilon = (1, 0, 2, 3, 4)$ is chosen, then:*

$$\rho_\varepsilon(\Gamma_{\hat{4}}(L, d)) = \rho_\varepsilon(\Lambda(L, d)) = s + 1.$$

Moreover, if dotted components are missing and m_α is the number of α -colored regions in a chess-board coloration of L (where α is the color of the unbounded region), then

$$\rho_\varepsilon(\tilde{\Omega}_{\hat{4}}(L, d)) = \rho_\varepsilon(\Omega(L, d)) = m_\alpha.$$

As already pointed out in Section 2.1, if $\partial M \cong \#_r(\mathbb{S}^1 \times \mathbb{S}^2)$, a Kirby diagram (L, d) of M also represents the closed 4-manifold \bar{M} uniquely obtained by adding r 3-handles and a 4-handle to the handle decomposition encoded by (L, d) .

Note that, if $r = 0$, then $\Gamma(L, d)$ is also a gem of \bar{M} (identified with M by capping off the spherical boundary). On the other hand, if $r > 0$, a gem of \bar{M} can be directly obtained from $\Gamma(L, d)$ in some particular cases, namely, for example, if $\Gamma(L, d)$ contains r ρ_3 -pairs whose switchings realize the attachment of the 3-handles.

More generally, we can state the following result:

Proposition 9 *Let M be a compact 4-manifold with $\partial M \cong \#_r(\mathbb{S}^1 \times \mathbb{S}^2)$ and let \bar{M} be its associated closed 4-manifold. If $\Gamma \in G_s^{(4)}$ is a gem of M such that $\Gamma_{\hat{4}}$ contains $r \geq 1$ ρ_3 -pairs of color $i \in \Delta_3$, whose switchings yield a gem of \mathbb{S}^3 , then:*

- (i) *if all ρ_3 -pairs of $\Gamma_{\hat{4}}$ are ρ_3 -pairs in Γ , too, then their switchings yield a gem of \bar{M} ;*
- (ii) *if $r' \leq r$ of them are ρ_4 -pairs in Γ , then by switching all pairs a gem of a closed 4-manifold N is obtained such that: $\bar{M} \cong \#_{r'}(\mathbb{S}^1 \times \mathbb{S}^3) \# N$.*

Proof. With regard to statement (i), let us first suppose $r = 1$ and let Γ' be the 5-colored graph obtained by switching the ρ_3 -pair of color $i \in \Delta_3$ in Γ . It is not difficult to see that Γ' represents a closed 4-manifold: in fact, $\Gamma'_{\hat{4}}$ represents the 3-sphere by hypothesis, while the only \hat{c} -residues that have been modified ($c \in \Delta_3$) still represent \mathbb{S}^3 since they are obtained by the corresponding \hat{c} -residues of Γ by switching a ρ_2 -pair (see Section 2.3).

Moreover, as shown in Figure 12, the switching of the ρ_3 -pair in Γ is equivalent to the insertion of a 4-colored edge on one of the edges of the pair, followed by the cancellation of a 3-dipole. It is not difficult to check that the insertion of the 4-colored edge has the topological effect of attaching a polyhedron homeomorphic to $\mathbb{D}^1 \times \mathbb{D}^3$ to the boundary of M , without affecting its interior: in fact, it corresponds to “breaking” a tetrahedral boundary face and inserting two 4-simplices sharing the 3-dimensional face opposite to the 4-labelled vertex, so as to change ∂M into a 3-sphere⁷. As a consequence, since the subsequent cancellation of the 3-dipole does not change the represented manifold (see Section 2.3), the closed 4-manifold $|K(\Gamma')|$ is obtained from M by attaching a 3-handle (and a 4-handle to cap off the resulting spherical boundary); by [25] Γ' is thus proved to represent \bar{M} .

The case $r > 1$ is proved in a similar way by induction, with the only difference that at each switching a $\mathbb{S}^1 \times \mathbb{S}^2$ summand is “subtracted” from the boundary (which is represented by the $\hat{4}$ -residue).

Let us now consider statement (ii) and start with the case $r = r' = 1$: let (e, f) be the ρ_4 -pair of color $i \in \Delta_3$ in Γ satisfying the hypotheses and Γ' the 5-colored graph obtained by switching (e, f) .

⁷The same argument is used in the proof of [11, Proposition 4.3] and also in [8, Proposition 11(ii)] for the particular case of gems arising from Kirby diagrams.

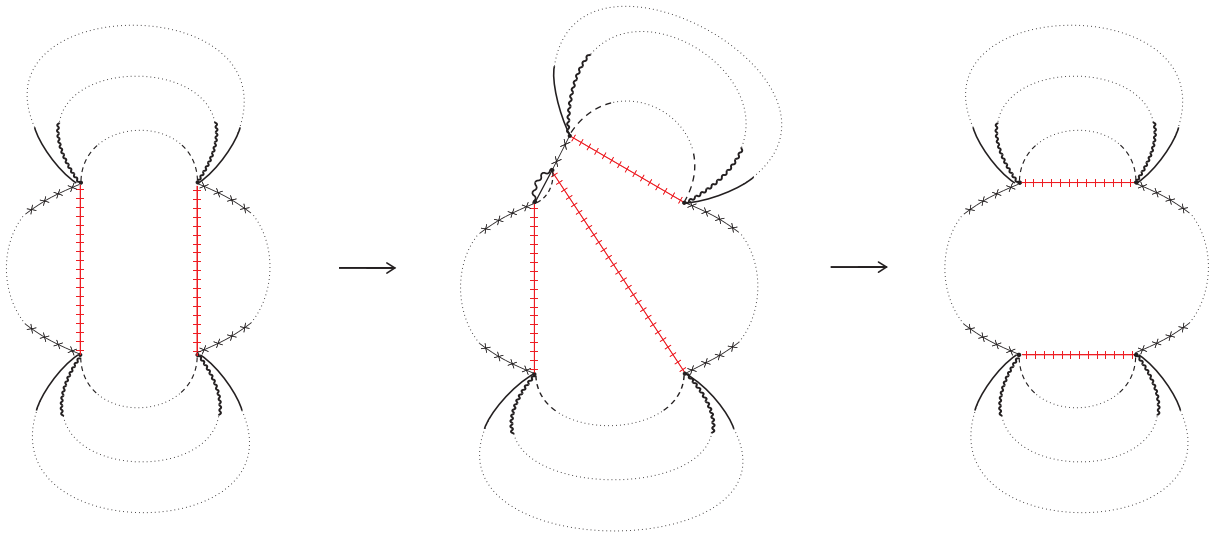


Figure 12: Factorization of the switching of a ρ_3 -pair

In order to recognize $|K(\Gamma')|$, we factorize the switching of (e, f) by some other combinatorial moves whose topological effects are known.

First, let us insert in Γ a 3-dipole, which does not change the represented manifold but has the effect of disconnecting the $\{i, 4\}$ -colored cycle C containing (e, f) . More precisely, let us delete an i -colored edge e' and a 4-colored edge f' of C , suitably chosen such that e and f belong to different connected components of $C \setminus \{e', f'\}$; then let us add two vertices, x and y , joined by three edges of the remaining colors, and connect x and y with the endpoints of e' (resp. f') by i -colored (resp. 4-colored) edges, taking care to respect the bipartition of the vertices. While the obtained 5-colored graph $\tilde{\Gamma}$ is still a gem of M , (e, f) is now a ρ_3 -pair in $\tilde{\Gamma}$ and it is not difficult to prove that it satisfies the hypotheses of the proposition⁸. Therefore, by statement (i), the switching of (e, f) in $\tilde{\Gamma}$ produces a new 5-colored graph $\tilde{\Gamma}'$ representing the closed manifold \bar{M} .

In order to recover Γ' , it is now necessary to delete the subgraph formed by x, y and paste the resulting hanging edges. However, this subgraph is a so-called *combinatorial handle* in $\tilde{\Gamma}'$, since x and y share the same $\{i, 4\}$ -colored cycle. As a consequence of [21, Theorem 7], Γ' turns out to be a gem of a closed 4-manifold N such that $\bar{M} \cong |K(\tilde{\Gamma}')| \cong (\mathbb{S}^1 \times \mathbb{S}^3) \# N$.

More generally, if $1 \leq r' \leq r$, we insert r' 3-dipoles in Γ in order to obtain a new gem $\tilde{\Gamma}$ of M containing r ρ_3 -pairs, then by switching them and deleting the r' resulting combinatorial handles, a 5-colored graph is obtained which, by the above arguments, is proved to represent a closed 4-manifold N such that, as claimed, $\bar{M} \cong \#_{r'}(\mathbb{S}^1 \times \mathbb{S}^3) \# N$. □

An example of the situations described in Proposition 9 (with $r = r' = 1$) can be seen in Figures 13 (statement (i)) and 14 (statement (ii)). More precisely, the left side of Figure 13 shows a gem of $\mathbb{S}^2 \times \mathbb{D}^2$, obtained by applying the algorithm to the 0-framed trivial knot, with the highlighted ρ_3 -pair, whose switching gives rise to the gem of the associated closed manifold \mathbb{S}^4 depicted on the right. A gem of $\mathbb{S}^1 \times \mathbb{D}^3$, obtained from a dotted trivial knot, can be seen on the left side of Figure 14, with a highlighted ρ_4 -pair whose switching produces the gem on the right representing $N (= \mathbb{S}^4)$, so that the associated closed 4-manifold is $(\mathbb{S}^1 \times \mathbb{S}^3) \# N$.

We conclude the Section by pointing out that useful applications of the described algorithm have been developed. In fact, it has been implemented by R.A. Burke in a software utility of *Regina* software package ([5]), which gives the additional advantage of allowing the manipulation of the resulting triangulations through an expressively thought-of heuristic for the 4-dimensional case.

⁸Note that $\tilde{\Gamma}_4$ is obtained from Γ_4 by the addition of the 3-dipole of vertices x and y .

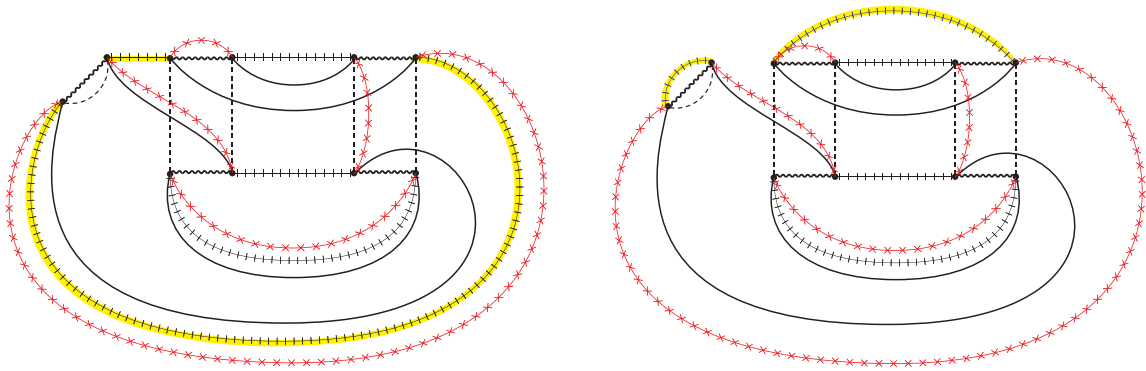


Figure 13: gems of $M = \mathbb{S}^2 \times \mathbb{D}^2$ (left) and $\bar{M} = \mathbb{S}^4$ (right), arising from the 0-framed trivial knot

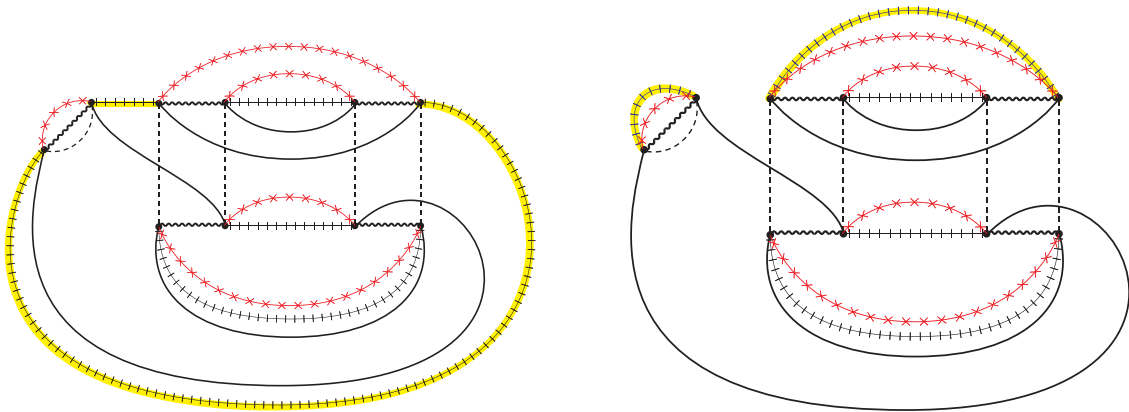


Figure 14: gems of $M = \mathbb{S}^1 \times \mathbb{D}^3$ (left) and $N(= \mathbb{S}^4)$ (right), so that $\bar{M} = (\mathbb{S}^1 \times \mathbb{S}^3) \# N$, arising from the dotted trivial knot

As a consequence, in [4], where a census of 4-manifold triangulations is studied, the algorithm is applied to get triangulations of the “canonical” PL-type of each topological type of the census, in order to perform automatically a comparison among the obtained triangulations.

Another interesting application regards the possibility of obtaining colored graphs - and hence colored triangulations - representing exotic pairs of compact PL 4-manifolds, i.e. pairs of 4-manifolds which are TOP-homeomorphic but not PL-homeomorphic. (Singular) triangulations of some exotic pairs are shown in both [8] and [3]; moreover, the first examples of triangulations of *corks* have been obtained in [3], where an initial analysis of the resulting triangulations is also presented, together with some interesting observations about particular configurations that seem to recur within.

3.2 From gems to trisections

In the last years, the notion of trisection has been extensively studied, also in its relationships with other manifold representation tools, such as handle-decompositions, Lefschetz fibrations, etc. In particular, in 2018, relying on the coincidence between DIFF and PL categories in dimension 4, Bell, Hass, Rubinstein and Tillmann ([2]) faced the study of trisections via (singular) triangulations.

They make use of a so-called *tricoloring*, i.e. a labelling of the vertices of each 4-simplex by three colors: in fact, the pull-back of the cubical structure of the standard 2-simplex, via the natural map induced by a tricoloring, gives rise to a subdivision of the 4-manifold in three 4-dimensional pieces. Under suitable conditions (always realized through Pachner moves, although at the cost of increasing the number of 4-simplices) the above subdivision turns out to be a trisection.

This approach - which moves trisections from SMOOTH to PL setting - brings all the advantages of a combinatorial description, and allows to algorithmically construct trisections and estimate their

genus, starting from singular triangulations.

Spreer and Tillmann ([34]) performed the first connection between trisections and gems, by applying the idea of Bell, Hass, Rubinstein and Tillmann to a special type of triangulations of simply-connected 4-manifolds, which contain exactly 5 vertices and one 1-simplex between each pair of vertices; their dual colored graphs are called *simple crystallizations*.

In this case, an obvious tricoloring of the vertices can be considered. Spreer and Tillmann proved that, for at least one simple crystallization of each 4-manifold among $\mathbb{C}\mathbb{P}^2$, $\mathbb{S}^2 \times \mathbb{S}^2$ and the $K3$ -surface, the associated subdivision is actually a trisection.

Moreover, they computed the genus of the central surface and pointed out that it had to be the minimum one, since in the case of simple crystallizations all 4-dimensional pieces of the subdivision are disks.

As a consequence, they completed the computation of the trisection genus for all the so-called “standard” simply-connected 4-manifolds, i.e. for the connected sums of $\mathbb{C}\mathbb{P}^2$ - possibly with reversed orientation -, $\mathbb{S}^2 \times \mathbb{S}^2$ and the $K3$ -surface; and for all such manifolds the trisection genus turns out to coincide with the second Betti number.

In this Section we will see how Spreer and Tillmann’s construction can be generalized, so as to yield trisections (directly or indirectly) from each colored triangulation of a closed 4-manifold, both in the orientable and non-orientable case. By the way, also compact 4-manifolds with connected boundary will be taken into consideration, by introducing a suitable extension of the notion of trisection to the boundary case (different from the one studied by Castro, Gay and Pinzon in [18]).

Note that, in order to study exotic structures, it is of fundamental importance to go beyond the class of simple crystallizations also in the simply-connected setting: in fact it is not difficult to prove the existence of infinitely many simply-connected PL 4-manifolds, TOP-homeomorphic to the same standard simply-connected PL 4-manifold, and not admitting simple crystallizations (see [7, Prop. 32]).

3.2.1 Gem-induced trisections

In [10] (resp. [11]), the ideas of [2] are applied to all colored triangulations of compact orientable (resp. non-orientable) 4-manifolds with empty or connected boundary, so as to generalize Spreer and Tillmann’s construction.

As a starting point, it is proved that each gem of a compact 4-manifold M with empty or connected boundary, both in the orientable and non-orientable case, induces a decomposition of M which “resembles” a trisection: there are three 4-dimensional “pieces”, two of which are handlebodies, while the third one is a collar of the boundary (or a 4-disk, if the boundary is empty); moreover, all these sub-manifolds intersect into a closed surface, but only two of the pairwise intersections are ensured to be 3-dimensional handlebodies.

Theorem 10 ([10], [11]) *For each 5-colored graph $\Gamma \in G_s^{(4)}$ representing a compact 4-manifold with empty (resp. connected boundary) M and for each cyclic permutation $\varepsilon = (\varepsilon_0, \varepsilon_1, \varepsilon_2, \varepsilon_3, \varepsilon_4 = 4)$ of Δ_4 , a triple $\mathcal{T}(\Gamma, \varepsilon) = (H_0, H_1, H_2)$ of submanifolds of M is constructed, such that*

- (a) $M = H_0 \cup H_1 \cup H_2$ and H_0, H_1, H_2 have pairwise disjoint interiors
- (b) H_1, H_2 are 4-dimensional handlebodies; H_0 is a 4-disk (resp. is homeomorphic to $\partial M \times [0, 1]$)
- (c) $H_{01} = H_0 \cap H_1$, $H_{02} = H_0 \cap H_2$ are 3-dimensional handlebodies
- (d) $\Sigma = H_0 \cap H_1 \cap H_2$ is a closed connected surface.

Moreover, if $H_{12} = H_1 \cap H_2$ is a 3-dimensional handlebody, too, then all the above handlebodies, as well as the surface Σ , are orientable or not according to the orientability of M ; in the first case Σ has genus $\rho_\varepsilon(\Gamma_{\hat{4}})$, while in the second one it has genus $2\rho_\varepsilon(\Gamma_{\hat{4}})$.

Sketch of the proof:

According to [2], for each tricoloring on the vertices of a triangulation, the possible trisecting submanifolds are obtained as pull-backs of the cubical structure of the standard 2-simplex, via the natural map induced by the tricoloring itself.

If the triangulation associated to a colored graph is considered, where all 4-simplices have one vertex of each color from 0 to 4, a tricoloring is easily obtained by giving color red to both the ε_0 - and ε_2 -labelled vertices, color green to both the ε_1 - and ε_3 -labelled vertices, and color blue to the vertex labelled by $\varepsilon_4 = 4$ (which can be actually assumed to be unique, since the boundary is either empty⁹ or connected: see Theorem 2).

Hence, one of the 4-dimensional pieces corresponds to the (truncated¹⁰) cone over the link of the unique blue vertex in the first barycentric subdivision of the triangulation (which is a 3-sphere in the closed case, and the boundary 3-manifold otherwise), while the other two are 4-dimensional handlebodies, obtained as regular neighbourhoods of the 1-dimensional subcomplexes of $K(\Gamma)$ generated by its red and green vertices, respectively.

As regards the pairwise intersections, which are 3-dimensional submanifolds, it is not difficult to prove that two of them meet any 4-simplex in triangular prisms, while the third (corresponding to the blue singleton) meets it in a cube. Moreover, any two of them meet in a unique square, and this square is exactly the intersection between the 4-simplex and the central surface.

See Figure 15 (redrawn from [34]), where ε is assumed to be the identity permutation: the vertices of the building blocks of the trisecting submanifolds, which are barycenters of faces, are indicated by the labels of the spanning vertices.

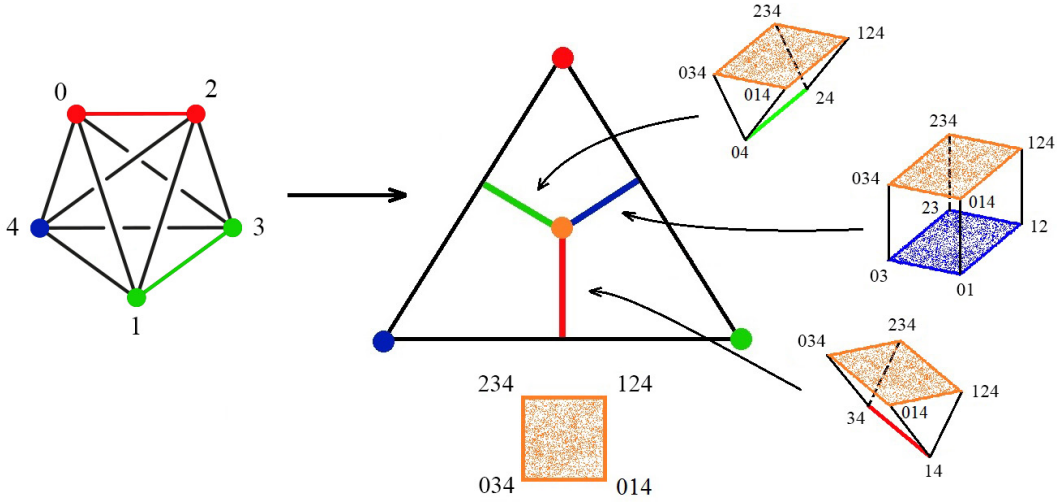


Figure 15: The intersections of the 3-dimensional pieces and the central surface of $\mathcal{T}(\Gamma, \varepsilon)$ with any 4-simplex

It is not difficult to check that both the triangular prisms corresponding to color red and those corresponding to color green always collapse to 1-dimensional subcomplexes, and hence are 3-dimensional handlebodies.

Moreover, the triple intersection $\Sigma = H_0 \cap H_1 \cap H_2$ is a closed connected surface, whose Euler characteristic can be easily computed. □

⁹Obviously, in the closed case, the role of color 4 can be played by any color c such that Γ_c is connected. In this paper, we always use 4 for simplicity, both in the closed and boundary case.

¹⁰Only in the boundary case, a small open neighbourhood of the singular (4-labelled) vertex has to be removed, according to gem theory.

Obviously, the construction is interesting when also the third 3-dimensional intersection turns out to be a handlebody, giving rise to an effective generalization to the connected boundary case of the notion of trisection, induced by graphs encoding manifolds:

Definition 8 ([10], [11]) Let M be a compact 4-manifold with empty or connected boundary. A *gem-induced trisection* of M is a decomposition $\mathcal{T}(\Gamma, \varepsilon) = (H_0, H_1, H_2)$ such that $H_{12} = H_1 \cap H_2$ is a 3-dimensional handlebody, $\Gamma \in G_s^{(4)}$ being a 5-colored graph representing M and $\varepsilon = (\varepsilon_0, \varepsilon_1, \varepsilon_2, \varepsilon_3, 4)$ a cyclic permutation of Δ_4 .

Remark 3 Note that, in the closed case, gem-induced trisections belong to a very significant type of trisections, where one of the pieces is a 4-disk. Such trisections have been widely studied, and are conjectured to exist for all closed simply-connected 4-manifolds: see, for example, [29], [24] and [30].

On the other hand, when the boundary is non-empty, the obtained decomposition of M is different from that introduced in [18], which is commonly intended as a trisection in the boundary case: in fact, it doesn't involve compression bodies and open book decompositions, but only handlebodies and Heegaard splittings, according to a suggestion by Rubinstein and Tillmann in [33, Section 4.5].

From the combinatorial point of view, a condition ensuring that a given gem admits a gem-induced trisection has been determined:

Proposition 11 ([10], [11]) *Let M be a compact 4-manifold with empty or connected boundary and $\Gamma \in G_s^{(4)}$ a gem of M of order $2p$; if there exists an ordering (e_1, \dots, e_p) of the 4-colored edges of Γ such that for each $j \in \{1, \dots, p\}$:*

$$\begin{aligned} & \text{there exists } i \in \Delta_3 \text{ such that all 4-colored edges of the} \\ & \{4, i\}\text{-colored cycle containing } e_j \text{ belong to the set } \{e_1, \dots, e_j\}, \end{aligned} \quad (*)$$

then $\mathcal{T}(\Gamma, \varepsilon)$ is a gem-induced trisection of M , for each cyclic permutation ε of Δ_4 .

Sketch of the proof:

It is easy to prove that the union of cubes, constituting the third 3-dimensional intersection $H_{12} = H_1 \cap H_2$ of $\mathcal{T}(\Gamma, \varepsilon)$, always collapses to the 2-dimensional complex $\overline{H}(\Gamma, \varepsilon)$ consisting of the union of their bottom faces. On the other hand, each such face corresponds to a 4-colored edge of Γ , and its edges are dual to bicolored cycles of Γ involving color 4.

In order to prove that, under the hypothesis of the statement, $\overline{H}(\Gamma, \varepsilon)$ further collapses to a graph, first note that condition (*), for $j = 1$, means that e_1 belongs, for a suitable color i , to a $\{4, i\}$ -colored cycle of Γ of length two; hence, the square in $\overline{H}(\Gamma, \varepsilon)$ corresponding to e_1 has a free edge from which it can be collapsed (see Figure 16, where ε is assumed to be the identity permutation).

Now, it is not difficult to check that an ordering of all 4-colored edges of Γ satisfying condition (*) corresponds exactly to a sequence of elementary collapses of all squares of $\overline{H}(\Gamma, \varepsilon)$.

□

It is worthwhile to note that gem-induced trisections fit Gay and Kirby's definition of trisection - hence allowing a direct estimation of the trisection genus - only for a suitable class of closed orientable 4-manifolds, characterized by admitting a handle decomposition with no 3-handles:

Proposition 12 [11] *Let M be a compact 4-manifold with empty or connected boundary. A gem-induced trisection of M is a trisection if and only if M is closed and orientable.*

Moreover, a closed orientable 4-manifold admits a gem-induced trisection if and only if it admits a handle decomposition lacking in 3-handles (or in 1-handles).

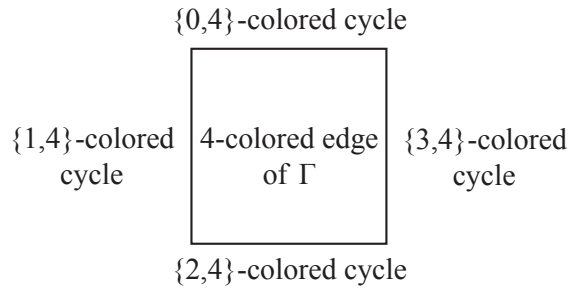


Figure 16: the square, corresponding to a 4-colored edge of Γ , constituting $\overline{H}(\Gamma, \varepsilon)$

The positive aspect of the above result is that the involved class possibly comprehends all simply-connected closed 4-manifolds, according to the famous Kirby problem n. 50 (see [27, Section 7.3]).

On the other hand, Proposition 12 shows that it is impossible to face the whole class of closed 4-manifolds, looking for an estimation of their trisection genus, directly via gem-induced trisections.

Nevertheless, starting from gem-induced trisections, two “indirect” approaches to trisections of closed (orientable and non-orientable) 4-manifolds can be applied, starting from gem-induced trisections. They will be the object of the following Sections.

3.2.2 First indirect approach

The first indirect approach to trisections of closed 4-manifolds via gem theory relies on the particular type of extension to the boundary case performed by gem-induced trisections, where one of the 4-dimensional pieces is a collar of the boundary. In fact, if the boundary of a compact 4-manifold M is homeomorphic to a connected sum of sphere bundles over \mathbb{S}^1 (both in the orientable and non-orientable case), it is not difficult to prove that any gem-induced trisection of M naturally gives rise to a trisection of the associated closed 4-manifold \overline{M} , i.e. the one uniquely obtained by gluing a 4-dimensional handlebody along ∂M , according to the already cited theorem by Laudenbach and Poenaru ([25]), together with its non-orientable version ([31]).

Since the intersecting surface is not affected, an upper bound for the trisection genus of the closed 4-manifold \overline{M} is obtained, through the so-called *G-trisection genus* of M (denoted by $g_{GT}(M)$), that is the minimum genus of a central surface in a gem-induced trisection:

Theorem 13 ([11]) *Let M be a compact orientable (resp. non-orientable) 4-manifold with boundary $\partial M \cong \#_m(\mathbb{S}^1 \otimes \mathbb{S}^2)$, $m > 0$. If M admits a gem-induced trisection, then $\overline{M} \cong M \cup \mathbb{Y}_m^{(\sim)}$ admits a trisection with the same central surface.*

As a consequence,

$$g_T(\overline{M}) \leq g_{GT}(M).$$

Definition 9 A trisection of a closed (orientable or non-orientable) 4-manifold \overline{M} is said to *arise from a colored triangulation* if it is either a gem-induced trisection of \overline{M} or is obtained from a gem-induced trisection of M (such that $\overline{M} \cong M \cup \mathbb{Y}_m^{(\sim)}$) according to Theorem 13.

In [10] and [11], various examples of closed 4-manifolds are shown, for which the estimation of the trisection genus via gems (either directly, through G-trisection genus, or indirectly through the trisection genus of an associated bounded manifold) is sharp. Moreover, since this type of estimation is proved to be subadditive with respect to connected sum, trisections arising from colored triangulations turn out to minimize the trisection genus for a wide class of (orientable and non-orientable) 4-manifolds:

Proposition 14 ([11]) *Let $\overline{M} \cong_{PL} (\#_p \mathbb{C}\mathbb{P}^2) \# (\#_{p'}(-\mathbb{C}\mathbb{P}^2)) \# (\#_q(\mathbb{S}^2 \times \mathbb{S}^2)) \# (\#_r K3) \# (\#_s(\mathbb{S}^1 \otimes \mathbb{S}^3)) \# (\#_t \mathbb{R}\mathbb{P}^4) \# (\#_u(\mathbb{S}^2 \times \mathbb{R}\mathbb{P}^2))$, with $p, p', q, r, s, t, u \geq 0$. Then, its trisection genus $g_T(\overline{M}) = (p + p' + 2q + 22r) + s + 2t + 3u$ is realized by a trisection arising from a colored triangulation.*

3.2.3 Second indirect approach

The second “indirect” approach to trisections via colored triangulations is used when the subdivision of the 4-manifold induced by a given gem has one of the 3-dimensional pieces (namely H_{12} , according to the notations of Section 3.2.1) that does not collapse to a graph.

In a recent paper by Martini and Toriumi ([28]), the idea of performing *stabilizations* along all edges of a fixed color is introduced, in order to obtain a trisection from each gem of a closed 4-manifold.

By translating their notations into those of Section 3.2.1, what they prove is that, by carving a regular neighborhood of a 4-colored edge \bar{e} ,¹¹ a 1-handle is added to H_0 , without affecting the 4-dimensional handlebodies H_1 and H_2 , while the genus of the intersecting surface Σ increases by one; with regard to the 3-dimensional pieces, the operation consists in adding a 1-handle to H_{01} and H_{02} , while adding a 2-handle to H_{12} . Figure 17 shows the effect of stabilization on the cubes that are building blocks of H_{12} , specifically on the pair of adjacent cubes corresponding to the 4-colored edge \bar{e} . In particular, in the middle square, which is part of the 2-dimensional spine $\bar{H}(\Gamma, \varepsilon)$ of H_{12} , a “hole” is created, which ensures the collapse of the square to its boundary.

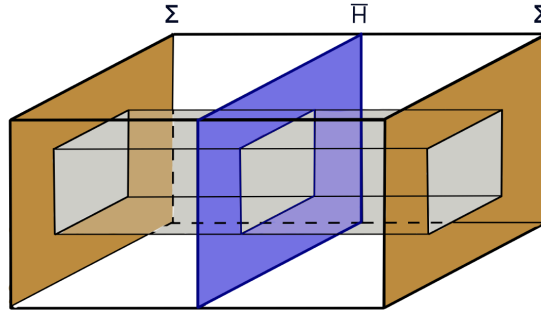


Figure 17: stabilization along a 4-colored edge

By performing the operation on every 4-colored edge of a gem $\Gamma \in G_s^{(4)}$, the collapse of $\bar{H}(\Gamma, \varepsilon)$ to a 1-dimensional subcomplex is guaranteed. In this way, Martini and Toriumi prove the existence of trisections arising from Γ , at the cost of increasing the genus of the central surface (since the final genus is the sum of the regular genus of $\Gamma_{\hat{4}}$ and the number of stabilizations).

In [12], the idea of Martini and Toriumi is applied to gems (belonging to $G_s^{(4)}$) representing compact 4-manifolds with empty or connected boundary, with the purpose of minimizing the number of stabilizations required to yield a trisection.

Both in the closed case and in the case of boundary homeomorphic to a connected sum of sphere bundles over \mathbb{S}^1 (when the first indirect approach to trisections can be applied), the genus of the obtained trisection turns out to be less or equal to the regular genus of the starting gem:

Theorem 15 ([12]) *Let $\Gamma \in G_s^{(4)}$ be a gem of a compact 4-manifold M with $\partial M \cong \#_m(\mathbb{S}^1 \otimes \mathbb{S}^2)$, $m \geq 0$. For each cyclic permutation ε of Δ_4 , the triple $\mathcal{T}(\Gamma, \varepsilon)$ gives rise to a trisection of $\bar{M} \cong M \cup \mathbb{Y}_m^{(\sim)}$ by applying k stabilizations, with $0 \leq k \leq \rho_\varepsilon(\Gamma) - \rho_\varepsilon(\Gamma_{\hat{4}})$. Hence:*

$$g_T(\bar{M}) \leq \rho_\varepsilon(\Gamma)$$

Sketch of the proof:

First, let us consider the (possibly disconnected) 3-colored graph $\Gamma_{\{\varepsilon_0, \varepsilon_3, \varepsilon_4=4\}}$, which regularly embeds in \mathbb{S}^2 (as happens for each 3-residue of a gem in dimension ≥ 3). This fact allows ordering all 4-colored edges of Γ , so that, after performing a stabilization along the first $g_{\varepsilon_0\varepsilon_3} - g_{\varepsilon_0\varepsilon_34}$ edges, the remaining ones satisfy condition (*) of Proposition 11.

¹¹Note that, if $\Gamma_{\hat{4}}$ is connected - as it is assumed in Section 3.2.1 - the case of 4-colored edges connecting distinct $\hat{4}$ -residues never occurs. On the contrary, Martini and Toriumi also take into account this situation, where carving along an edge simply corresponds to a connected sum of “pieces” of the decomposition.

Further, well-known combinatorial formulas in gem theory (see for example [9, Proposition 3.1]) enable to check that $g_{\varepsilon_0\varepsilon_3} - g_{\varepsilon_0\varepsilon_34} = \rho_\varepsilon(\Gamma) - \rho_\varepsilon(\Gamma_{\hat{4}})$.

Hence, a gem-induced trisection of M is obtained, with central surface of genus: $\rho_\varepsilon(\Gamma_{\hat{4}}) + (\rho_\varepsilon(\Gamma) - \rho_\varepsilon(\Gamma_{\hat{4}}))$. Finally, the thesis concerning \bar{M} follows, by possible application of Theorem 13 (in case $m > 0$).

□

As a direct consequence, the following statement holds:

Theorem 16 ([12]) *For each compact 4-manifold M with $\partial M \cong \#_m(\mathbb{S}^1 \otimes \mathbb{S}^2)$, $m \geq 0$, then:*

$$g_T(\bar{M}) \leq \mathcal{G}(M)$$

where $\bar{M} \cong M \cup \mathbb{Y}_m^{(\sim)}$.

In particular, in the closed case, the regular genus turns out to be an upper bound for the trisection genus:

Theorem 17 ([12]) *For each closed 4-manifold M , then:*

$$g_T(M) \leq \mathcal{G}(M).$$

3.3 From Kirby diagrams to trisections via gems

In the present Section, we will show how the results and constructions in Section 3.2 take advantage of those of Section 3.1, as regards the computation of the trisection genus of each closed orientable 4-manifold.

The starting point is the fact, proved in [10], that all 5-colored graphs obtained through the algorithmic construction described in Section 3.1, starting from Kirby diagrams (see Theorem 5), as well as the simplified ones arising from framed links (see Theorem 7), admit gem-induced trisections:

Theorem 18 ([10]) *Let M be a compact 4-manifold with empty or connected boundary admitting a handle decomposition with no 3-handles.*

Then, from each (connected and with dotted components in “good position”) Kirby diagram (L, d) of M , a gem-induced trisection of M can be algorithmically constructed, whose central surface has genus $s + 1$, s being the crossing number of the chosen diagram.

Furthermore, if (L, d) has no dotted components (equivalently, if 1-handles are missing, too), then a gem-induced trisection of M can be obtained, whose central surface has genus m_α , where m_α is the number of α -colored regions in a chess-board coloration of the diagram, α being the color of the unbounded region.

Sketch of the proof:

The combinatorial properties of the graphs obtained through the constructions of Section 3.1 always allow ordering the set of their 4-colored edges, so as to satisfy the collapsing condition (*) of Proposition 11.

With regard to the graph $\Gamma(L, d)$, it is sufficient to consider the following sequence:

- for increasing values of $j \in \{m + 1, \dots, l\}$, the triad of edges between vertices P_{2r} and P_{2r+1} , for $r = 0, 1, 2$, of the quadricolor Q_j , followed by the 4-colored edges corresponding to the sequence of highlighted segments of arcs on the j -th (framed) component, and finally by the other 4-colored edges as they are met along that component;

- for each $j \in \{1, \dots, m\}$, all 4-colored edges corresponding to the j -th dotted component, in any order, except those of the $\{1, 4\}$ -cycle containing v_j and v'_j , then the 4-colored edge between v_j and v'_j , and finally the remaining 4-colored edge.

As regards the 5-colored graph $\tilde{\Omega}(L, d)$ (whose $\hat{4}$ -residue is obtained from that of $\Gamma(L, d)$, when dotted components are missing, via generalized dipole eliminations), it is sufficient to consider, for increasing values of $j \in \{1, \dots, l\}$, first the triad of edges between vertices P_{2r} and P_{2r+1} , for $r = 0, 1, 2$, of the quadricolor Q_j , and then the other 4-colored edges as they are met along the j -th component.

Hence, in both cases, a gem-induced trisection exists, whose genus can be directly computed via Proposition 8.

□

As a consequence, an estimation of the trisection genus $g_T(\bar{M})$ is obtained for each closed orientable 4-manifold \bar{M} , in terms of the combinatorial properties of a Kirby diagram representing it.

Theorem 19 ([11])

(i) For each closed orientable 4-manifold \bar{M} ,

$$g_T(\bar{M}) \leq s + 1,$$

s being the crossing number of a (connected and with dotted components in “good position”) Kirby diagram representing \bar{M} .

(ii) Furthermore, if \bar{M} admits a handle decomposition lacking in 1-handles, then

$$g_T(\bar{M}) \leq m_\alpha,$$

where m_α is the number of α -colored regions in a chess-board coloration of a (connected and with no dotted component) Kirby diagram representing \bar{M} , α being the color of the unbounded region.

Sketch of the proof:

As recalled in Section 2.1, if (L, d) is a Kirby diagram (with the required properties as regards connectedness and “good position” of 1-handles) representing \bar{M} , (L, d) also represents the compact 4-manifold M consisting only of the union of the 0-, 1- and 2-handles of the associated handle-decomposition.

Now, Theorem 18 ensures the existence of a gem-induced trisection of M whose central surface has genus $s + 1$ (or, better, m_α if (L, d) contains no dotted component).

Hence, the thesis follows from Theorem 13.

□

In case of disconnected Kirby diagrams, instead of performing Reidemeister moves in order to apply Theorem 19, it is also possible to take advantage of the well-known fact that the represented compact 4-manifold is the boundary connected sum of the ones represented by each connected component. As a consequence, by repeated application of Theorem 19 (statement (i) or (ii), according to the case), together with subadditivity of the genus of trisections arising from gems (see [11, Proposition 3.8(iv)] and the proof of [11, Proposition 4.4]), the following result can be stated:

Corollary 20 ([11]) *Let \bar{M} be a closed orientable 4-manifold and (L, d) a Kirby diagram of \bar{M} with c connected components and whose dotted components - if any - are in good position. Then:*

(i)

$$g_T(\bar{M}) \leq s + c,$$

s being the crossing number of (L, d) .

(ii) Furthermore, if (L, d) has no dotted components, then

$$g_T(\bar{M}) \leq m_\alpha + c - 1,$$

where m_α is the number of α -colored regions in a chess-board coloration of (L, d) , α being the color of the unbounded region.

3.3.1 From framed links to trisection diagrams via gems

In [28], Martini and Toriumi analyze the decomposition generated by their procedure to yield trisections from any gem, and point out that it gives rise to a collection of trisection diagrams of the appropriate genus, since they obtain a redundant amount of attaching curves of the 3-dimensional intersections: see [28, Section 4.6] for details.

By adapting the idea of Martini and Toriumi to the case of a gem Γ satisfying condition (*) of Proposition 11 (and therefore admitting a gem-induced trisection $\mathcal{T}(\Gamma, \varepsilon)$), a trisection diagram can actually be identified on the central surface of the induced trisection, which turns out to coincide with the embedding surface $F_\varepsilon(\Gamma_{\hat{4}})$ of the graph without color 4. $F_\varepsilon(\Gamma_{\hat{4}})$ has genus $\rho_\varepsilon(\Gamma_{\hat{4}})$ in the orientable case and $2\rho_\varepsilon(\Gamma_{\hat{4}})$ in the non-orientable one, and the systems of curves drawn on it and constituting a trisection diagram are nothing but suitable bicolored cycles of the given gem.

This procedure succeeds not only in the closed case, but also in the case of boundary homeomorphic to a connected sum of sphere bundles of \mathbb{S}^1 , where the gem-induced trisection of the bounded 4-manifold M uniquely identifies - according to Section 3.2.2 - a trisection of the associated closed 4-manifold \bar{M} .

Proposition 21 *Let $\Gamma \in G_s^{(4)}$ be a gem of a compact 4-manifold M with $\partial M \cong \#_m(\mathbb{S}^1 \otimes \mathbb{S}^2)$, $m \geq 0$, satisfying condition (*) of Proposition 11.*

Then, for each cyclic permutation $\varepsilon = (\varepsilon_0, \varepsilon_1, \varepsilon_2, \varepsilon_3, 4)$ of Δ_4 , a trisection diagram for the associated closed 4-manifold \bar{M} is given by the following three systems of curves $\{\alpha, \beta, \gamma\}$ on $F_\varepsilon(\Gamma_{\hat{4}})$:

- *the α curves (resp. β curves) consist of all $\{\varepsilon_0, \varepsilon_2\}$ -colored cycles (resp. $\{\varepsilon_1, \varepsilon_3\}$ -colored cycles) of Γ , but those corresponding to a maximal tree of the 1-dimensional subcomplex $K_{\varepsilon_1\varepsilon_3}$ (resp. $K_{\varepsilon_0\varepsilon_2}$), generated by the vertices labelled ε_1 and ε_3 (resp. ε_0 and ε_2) of $K(\Gamma)$.*
- *the γ curves are a subset of the $\{c, 4\}$ -colored cycles of Γ , with $c \in \Delta_3$, which can be combinatorially identified by following - via condition (*) - the collapsing sequence of the 3-dimensional handlebody H_{12} (according to the notations of Section 3.2.1).*

Proof. According to Theorem 10, the gem-induced trisection $\mathcal{T}(\Gamma, \varepsilon)$ of M is formed by the triple (H_0, H_1, H_2) , where H_1 (resp. H_2) is a regular neighbourhood of $K_{\varepsilon_0\varepsilon_2}$ (resp. $K_{\varepsilon_1\varepsilon_3}$), while H_0 is either the 4-disk obtained by coning over the triangulation $K(\Gamma_{\hat{4}})$ of the 3-sphere (if $m = 0$) or a collar of the triangulation $K(\Gamma_{\hat{4}})$ of $\partial M \cong \#_m(\mathbb{S}^1 \otimes \mathbb{S}^2)$ (if $m > 0$).

Moreover, in case $m > 0$, $\mathcal{T}(\Gamma, \varepsilon)$ naturally gives rise - according to Theorem 13 - to a trisection $\bar{\mathcal{T}} = (\hat{H}_0, H_1, H_2)$ of the closed 4-manifold $\bar{M} \cong M \cup \mathbb{Y}_m^{(\sim)}$, where $\hat{H}_0 = H_0 \cup \mathbb{Y}_m^{(\sim)}$, with the same central surface Σ as $\mathcal{T}(\Gamma, \varepsilon)$.

It is not difficult to check that, both in the case $m = 0$ (where we define $\bar{\mathcal{T}} = \mathcal{T}(\Gamma, \varepsilon)$ for sake of notational simplicity) and in the case $m > 0$, the trisection $\bar{\mathcal{T}}$ is completely identified by the attachments on Σ of $H_{01} = H_0 \cap H_1 = \hat{H}_0 \cap H_1$, $H_{02} = H_0 \cap H_2 = \hat{H}_0 \cap H_2$ and $H_{12} = H_1 \cap H_2$ (which are 3-dimensional handlebodies by hypothesis). Now, as pointed out by Martini and Toriumi¹², the quadrangulation of the central surface Σ given by the union of the ‘‘orange’’ squares in Figure 15 is dual to the cellular subdivision of the embedding surface $F_\varepsilon(\Gamma_{\hat{4}})$, given by $\Gamma_{\hat{4}}$ itself. Hence, Σ and $F_\varepsilon(\Gamma_{\hat{4}})$ can be identified. Moreover, the set of $\{\varepsilon_0, \varepsilon_2\}$ -colored cycles (resp. $\{\varepsilon_1, \varepsilon_3\}$ -colored cycles) of Γ can be seen as projections on Σ of meridian curves of the 3-dimensional handlebody H_{01} (resp.

¹²See [28, Paragraph 4.6], and in particular the caption of Figure 17.

H_{02}): in fact, $\{\varepsilon_0, \varepsilon_2\}$ -colored cycles (resp. $\{\varepsilon_1, \varepsilon_3\}$ -colored cycles) of Γ exactly correspond to the union of the red (resp. green) edges to which each prism constituting H_{01} (resp. H_{02}) collapses (see Figure 15 and [28, Paragraph 4.6]). Hence, the statement regarding α and β curves easily follows, by noting that a system of (independent) curves realizing the attachment of H_{01} (resp. H_{02}) can be obtained from the set of such red (resp. green) edges by shrinking to a point the ones belonging to a maximal tree.

As regards H_{12} , note that it always collapses to the 2-dimensional complex $\bar{H}(\Gamma, \varepsilon)$, consisting of a square for each 4-colored edge of Γ , since in the cubical intersection of H_{12} with any 4-simplex the face belonging to the central surface is free: see the proof of Proposition 11, together with Figures 15 and 16.

Moreover, by hypothesis, $\bar{H}(\Gamma, \varepsilon)$ further collapses to a 1-dimensional complex via the collapsing sequence given by the ordering (e_1, \dots, e_p) of 4-colored edges satisfying condition (*), as described in the proof of Proposition 11. Hence, a spine of H_{12} consists of the set of edges of $\bar{H}(\Gamma, \varepsilon)$ remaining at the end of the collapsing sequence, and a system of (independent) curves realizing the attachment of H_{12} can be obtained from this set of edges by shrinking to a point the ones belonging to a maximal tree. Since each edge of $\bar{H}(\Gamma, \varepsilon)$ corresponds to a $\{c, 4\}$ -colored cycle of Γ , with $c \in \Delta_3$, and can be projected on Σ by reversing the collapse of each cube of H_{12} to its bottom face, the statement regarding the γ curves follows. □

Example 1 Figures 18 and 19 show how to apply Proposition 21: the gem of $\mathbb{S}^2 \times \mathbb{S}^2$ in Figure 18 admits the depicted ordering of its 4-colored edges, $(e_1, e_2, e_3, e_4, e_5, e_6, e_7)$, which corresponds to a sequence of collapses of the squares of $\bar{H}(\Gamma, \varepsilon)$ (ε being the identity permutation) from their free edges corresponding respectively to $\{c_i, 4\}$ -colored cycles, $\forall i = 1, \dots, 7$ (with $c_1 = 1, c_2 = 1, c_3 = 3, c_4 = 2, c_5 = 3, c_6 = 2, c_7 = 1$). The result is a 1-dimensional complex \bar{H} consisting only of five edges: three corresponding to all $\{0, 4\}$ -colored cycles of Γ , one corresponding to the $\{2, 4\}$ -colored cycle containing $\{e_1, e_2, e_5, e_7\}$ and one corresponding to the $\{3, 4\}$ -colored cycle containing $\{e_2, e_4, e_6, e_7\}$.

By shrinking to a point one of the edges of \bar{H} corresponding to a $\{0, 4\}$ -colored cycle (for example the one containing e_2, e_5 and e_4), and both edges corresponding to $\{2, 4\}$ - and $\{3, 4\}$ -colored cycles, the system γ of curves depicted in red in Figure 19 is identified; it gives rise to a trisection diagram of $\mathbb{S}^2 \times \mathbb{S}^2$, together with the system α of curves depicted in green (all $\{0, 2\}$ -colored cycles of Γ , but one arbitrarily chosen, since $K_{\varepsilon_1 \varepsilon_3}$ contains exactly two vertices) and the system β of curves depicted in blue (all $\{1, 3\}$ -colored cycles of Γ , but one arbitrarily chosen, since $K_{\varepsilon_0 \varepsilon_2}$ contains exactly two vertices).

Note that the three systems of curves on the (genus two) surface where Γ_4 regularly embeds, in pairs give rise to genus two Heegaard diagrams of the boundaries of the 4-dimensional pieces of the trisection of $\mathbb{S}^2 \times \mathbb{S}^2$ (which are actually 3-spheres).

Let us now consider a (connected) framed link (L, d) , with l components, representing a closed 4-manifold \bar{M} and let M be the compact 4-manifold such that \bar{M} is obtained from M by adding a suitable number of 3-handles. In virtue of Proposition 19, the procedure described in Proposition 21 can be applied to both the gem $\Gamma(L, d)$ of M and the gem $\hat{\Omega}(L, d)$ obtained from $\Gamma(L, d)$ via generalized dipole eliminations (see Section 3.1).

In this case, the three systems of curves of the associated trisection diagram are drawn on the closed orientable surface Σ where $\Gamma_4(L, d)$ (resp. $\hat{\Omega}_4(L, d)$) regularly embeds, whose genus is $s + 1$, s being the crossing number of L (resp. is m_α , where m_α is the number of α -colored regions in a chess-board coloration of L , α being the color of the unbounded region), according to Proposition 8. Moreover, each system of curves is simply obtained from the cycles of a suitable pair of colors of $\Gamma(L, d)$ (resp. $\hat{\Omega}(L, d)$):

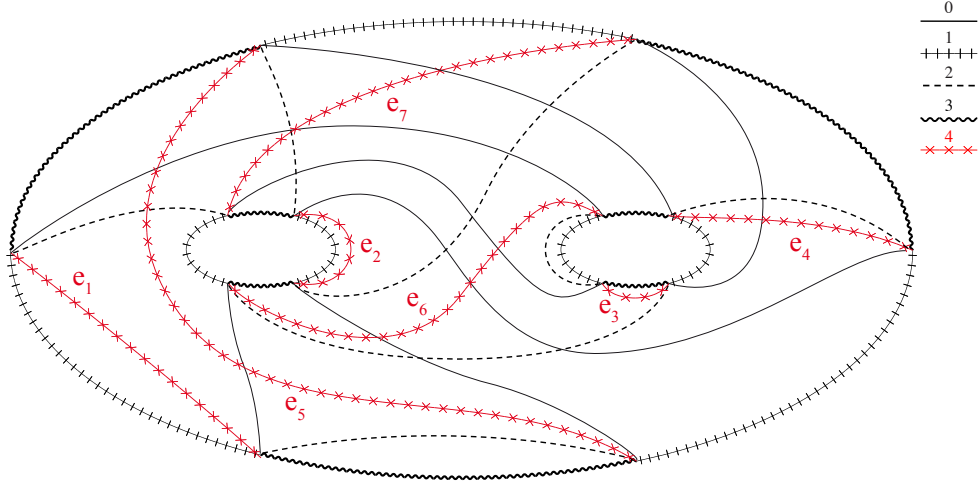


Figure 18: A gem of $\mathbb{S}^2 \times \mathbb{S}^2$, with an ordering of 4-colored edges giving rise to a gem-induced trisection

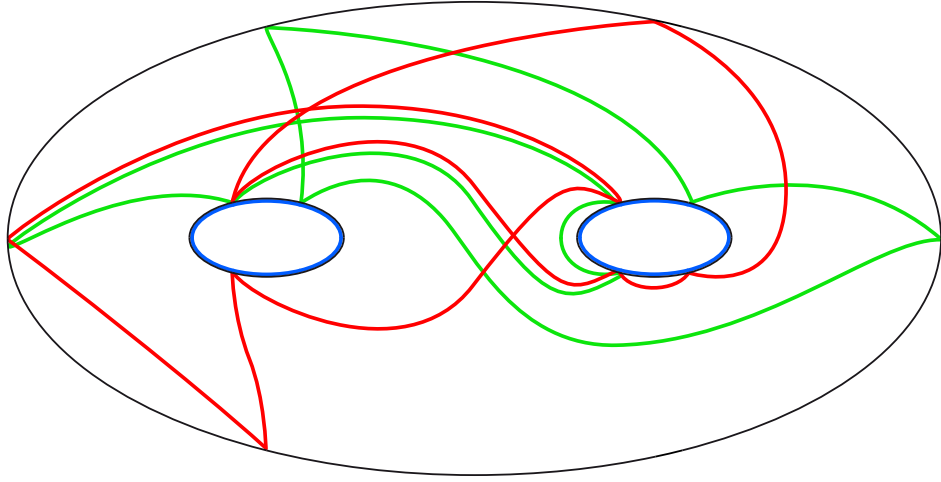


Figure 19: The associated trisection diagram of $\mathbb{S}^2 \times \mathbb{S}^2$

Proposition 22 *With the above notations, let \mathcal{T} be the trisection of \bar{M} induced by $\Gamma(L, d)$ (resp. $\tilde{\Omega}(L, d)$). Then, a trisection diagram for \mathcal{T} is given by the following three system of curves $\{\alpha, \beta, \gamma\}$ on Σ :*

- the α curves are all $\{1, 2\}$ -colored cycles of $\Gamma(L, d)$ (resp. $\tilde{\Omega}(L, d)$), but one arbitrarily chosen;
- the β curves are all $\{0, 3\}$ -colored cycles of $\Gamma(L, d)$ (resp. $\tilde{\Omega}(L, d)$), but $2l - 1$ corresponding to a maximal tree of the 1-dimensional subcomplex K_{12} generated by the vertices labelled 1 and 2;
- the γ curves are all $\{2, 4\}$ -colored cycles of $\Gamma(L, d)$ (resp. $\tilde{\Omega}(L, d)$), but one arbitrarily chosen.

Proof. Proposition 8 ensures that, if the permutation $\varepsilon = (1, 0, 2, 3, 4)$ of Δ_4 is chosen, then $\rho_\varepsilon(\Gamma_4(L, d)) = \rho_\varepsilon(\Lambda(L, d)) = s + 1$ (resp. $\rho_\varepsilon(\tilde{\Omega}_4(L, d)) = \rho_\varepsilon(\Omega(L, d)) = m_\alpha$). Moreover, by construction, all 4-colored edges of $\Gamma(L, d)$ (resp. $\tilde{\Omega}(L, d)$) double 1-colored edges of $\Gamma_4(L, d) = \Lambda(L, c)$ (resp. of $\tilde{\Omega}_4(L, d) = \Omega(L, d)$), but the $3l$ ones added between the vertices $P_{2r}^{(i)}$ and $P_{2r+1}^{(i)}$, for $r = 0, 1, 2$, of the quadricolor Q_i (Q_i being the quadricolor corresponding to the “cut” X_i on the i -th component of L , $\forall i \in \{1, 2, \dots, l\}$).

Let us now consider the following ordering of all 4-colored edges $\Gamma(L, d)$ (resp. $\tilde{\Omega}(L, d)$):

- first, in any order, all 4-colored edges belonging to $\{1, 4\}$ -colored cycles of length two, together with the l 4-colored edges between the vertices $P_0^{(i)}$ and $P_1^{(i)}$, $\forall i \in \{1, 2, \dots, l\}$ (which belong to $\{0, 4\}$ -colored cycles of length two);
- then, the l 4-colored edges between the vertices $P_4^{(i)}$ and $P_5^{(i)}$, $\forall i \in \{1, 2, \dots, l\}$;
- finally, the l 4-colored edges between the vertices $P_2^{(i)}$ and $P_3^{(i)}$, $\forall i \in \{1, 2, \dots, l\}$.

It is not difficult to check that the above ordering - which satisfies condition (*) of Proposition 11 - corresponds to a collapsing sequence of all squares of the 2-dimensional complex $\bar{H}(\Gamma, \varepsilon)$, giving rise to a 1-dimensional spine \bar{H} of H_{12} which consists of the edges corresponding to:

- all $\{2, 4\}$ -colored cycles of $\Gamma(L, d)$ (resp. $\tilde{\Omega}(L, d)$)
- all $\{0, 4\}$ -colored cycles of $\Gamma(L, d)$ (resp. $\tilde{\Omega}(L, d)$), but those containing $P_0^{(i)}$ and $P_1^{(i)}$, $\forall i \in \{1, 2, \dots, l\}$
- all $\{3, 4\}$ -colored cycles of $\Gamma(L, d)$ (resp. $\tilde{\Omega}(L, d)$), but those containing $P_4^{(i)}$ and $P_5^{(i)}$, $\forall i \in \{1, 2, \dots, l\}$.

Moreover, the combinatorial structure of $\Gamma(L, d)$ and $\tilde{\Omega}(L, d)$ ensures that all edges of \bar{H} corresponding to $\{0, 4\}$ -colored (resp. $\{3, 4\}$ -colored) cycles have a free end-point, since the corresponding cycles belong to disjoint $\{0, 1, 4\}$ -residues (resp. $\{1, 3, 4\}$ -residues). Hence, \bar{H} further collapses to a 1-dimensional subcomplex, whose edges correspond to all $\{2, 4\}$ -colored cycles of $\Gamma(L, d)$ (resp. $\tilde{\Omega}(L, d)$).

On the other hand, all these edges have the same end-points, since $\Gamma(L, d)$ (resp. $\tilde{\Omega}(L, d)$) contains exactly one $\{0, 2, 4\}$ -residue and exactly one $\{2, 3, 4\}$ -residue (see the proof of [6, Theorem 2], ensuring that $\Lambda_j(L, d)$, and hence $\Omega_j(L, d)$, is connected, for $j \in \{0, 3\}$). The statement concerning the γ curves now directly follows.

Finally, the statement concerning the α (resp. β) curves is a consequence of the analogue general statement of Proposition 21, together with the fact that both $\Gamma_4(L, d) = \Lambda(L, d)$ and $\tilde{\Omega}_4(L, d) = \Omega(L, d)$ have exactly one $\hat{0}$ -residue and one $\hat{3}$ -residue (resp. exactly l $\hat{1}$ -residue and l $\hat{2}$ -residue), according to the proof of [6, Theorem 2].

□

Finally, we point out that our particular extension to the boundary case of the notion of trisection, given by gem-induced trisections, suggests also a possible extension of the notion of trisection diagram to simply-connected compact 4-manifolds with connected boundary.

Definition 10 A *G-trisection diagram* of genus g is a 4-tuple $(\Sigma; \alpha, \beta, \gamma)$, where Σ is a genus g orientable surface and α, β, γ are complete systems of curves on Σ , such that:

- $(\Sigma; \alpha, \gamma)$ and $(\Sigma; \beta, \gamma)$ are (genus g) Heegaard diagrams of $\#_{k_1}(\mathbb{S}^1 \times \mathbb{S}^2)$ and $\#_{k_2}(\mathbb{S}^1 \times \mathbb{S}^2)$ respectively, with $0 \leq k_i \leq g$, for $i = 1, 2$;
- $(\Sigma; \alpha, \beta)$ is a (genus g) Heegaard diagram of a closed connected 3-manifold.

Proposition 23 *Let M be a simply-connected compact 4-manifold with connected boundary, admitting a genus g gem-induced trisection. Then, M is uniquely identified by a G-trisection diagram $(\Sigma; \alpha, \beta, \gamma)$ of genus g , so that $(\Sigma; \alpha, \beta)$ is a Heegaard diagram of ∂M .*

Proof. Let $\mathcal{T} = (H_0, H_1, H_2)$ be a triple of submanifolds of M constituting a gem-induced trisection. By definition, H_1 and H_2 are 4-dimensional handlebodies, while H_0 is a collar of ∂M ; moreover, all pairwise intersections are 3-dimensional handlebodies, while $\Sigma = H_0 \cap H_1 \cap H_2$ is a closed orientable genus g surface. If α, β, γ are attaching curves on Σ of $H_{01} = H_0 \cap H_1$, $H_{02} = H_0 \cap H_2$ and $H_{12} = H_1 \cap H_2$ respectively, then $(\Sigma; \alpha, \beta, \gamma)$ turns out to be a G-trisection diagram (see [10, Remark 15] for details).

On the other hand, given such a G-trisection diagram, let W be the compact 4-manifold obtained by attaching a collar of two genus g 3-dimensional handlebodies (corresponding to H_{01} e H_{02}) to $\Sigma \times \mathbb{D}^2$ according to the curves α and β respectively, in full analogy of the procedure described after Definition 2. Since M is obtained from W by adding 3-handles (corresponding to H_1 and H_2), and M is simply-connected with connected boundary by hypothesis, Theorem 1 in [35] ensures that W (or, equivalently, the G-trisection diagram) uniquely determines M .

□

As a consequence, the following statement easily follows from Proposition 21, by adapting the same proving arguments to the (general) boundary case:

Proposition 24 *Let $\Gamma \in G_s^{(4)}$ be a gem of a simply-connected compact 4-manifold M with connected boundary ∂M , satisfying condition (*) of Proposition 11.*

Then, for any cyclic permutation ε of Δ_4 , a G-trisection diagram for M is given by the following three system of curves $\{\alpha, \beta, \gamma\}$ on $F_\varepsilon(\Gamma_4)$:

- *the α curves (resp. β curves) consist of all $\{\varepsilon_0, \varepsilon_2\}$ -colored cycles (resp. $\{\varepsilon_1, \varepsilon_3\}$ -colored cycles) of Γ , but those corresponding to a maximal tree of the 1-dimensional subcomplex $K_{\varepsilon_1 \varepsilon_3}$ (resp. $K_{\varepsilon_0 \varepsilon_2}$), generated by the vertices labelled ε_1 and ε_3 (resp. ε_0 and ε_2) of $K(\Gamma)$.*
- *the γ curves are a subset of $\{c, 4\}$ -colored cycles of Γ , with $c \in \Delta_3$, which can be combinatorially identified by following - via condition (*) - the collapsing sequence for the 3-dimensional handlebody H_{12} (according to the notations of Section 3.2.1).*

Also Proposition 22 can be extended to the case of (connected) framed links representing 4-manifolds with boundary:

Proposition 25 *Let (L, d) be a (connected) framed link representing a (simply-connected) 4-manifold M with non-empty boundary, and let \mathcal{T} be the gem-induced trisection of M induced by $\Gamma(L, d)$ (resp. $\tilde{\Omega}(L, d)$). Then, a G-trisection diagram for \mathcal{T} is given by the following three system of curves $\{\alpha, \beta, \gamma\}$ on Σ :*

- *the α curves are all $\{1, 2\}$ -colored cycles of $\Gamma(L, d)$ (resp. $\tilde{\Omega}(L, d)$), but one arbitrarily chosen;*
- *the β curves are all $\{0, 3\}$ -colored cycles of $\Gamma(L, d)$ (resp. $\tilde{\Omega}(L, d)$), but $2l - 1$ corresponding to a maximal tree of the 1-dimensional subcomplex K_{12} generated by the vertices labelled 1 and 2;*
- *the γ curves are all $\{2, 4\}$ -colored cycles of $\Gamma(L, d)$ (resp. $\tilde{\Omega}(L, d)$), but one arbitrarily chosen.*

Example 2 Figures 20 and 21 show an application of Proposition 25 to the framed link consisting of a trefoil knot K_T with framing 1: the gem $\tilde{\Omega}(K_T, 1)$ of Figure 20 represents a (simply-connected) compact 4-manifold M (whose boundary is the Poincaré homology sphere), has regular genus $m_\alpha + 1 = 3$ and gives rise to a gem-induced trisection of genus $m_\alpha = 2$. The associated G-trisection diagram is depicted in Figure 21. Note that by considering blue and yellow (resp. blue and green) curves, a genus two Heegaard diagram of the boundary of one of the 4-dimensional handlebody of the trisection of M is obtained, while yellow and green curves give rise to a genus two Heegaard diagram of the Poincaré homology sphere.

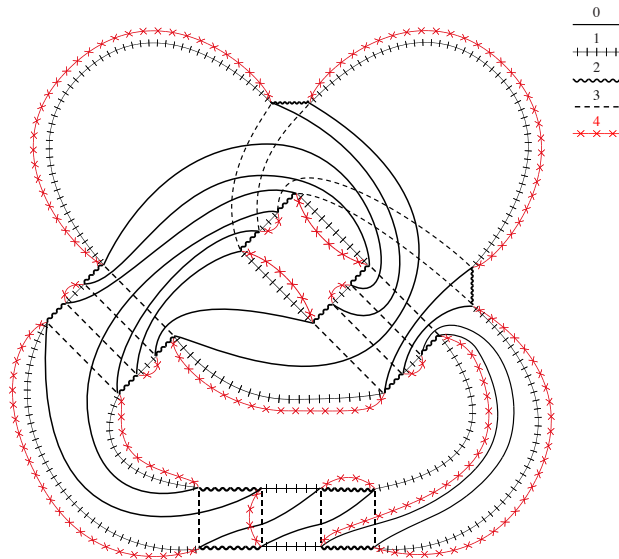


Figure 20: the gem $\tilde{\Omega}(K_T, 1)$, K_T being the trefoil knot

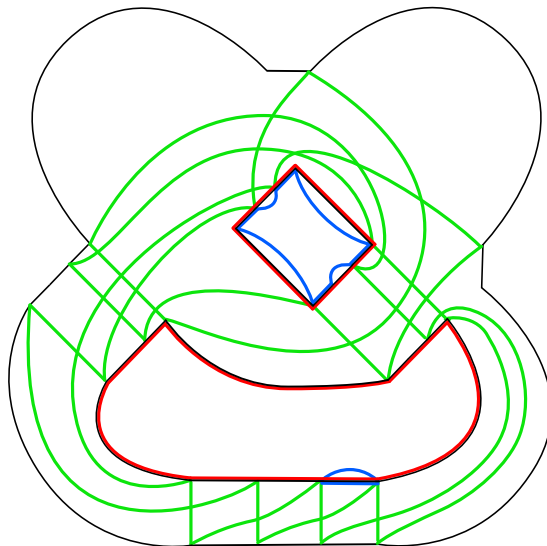


Figure 21: the G-trisection diagram arising from $\tilde{\Omega}(K_T, 1)$

4 Open problems and trends

The constructions and results presented in the previous Sections show the strong relationship which exists among the three involved representations for PL 4-manifolds, namely Kirby diagrams, trisections and gems, pointing out how the latter can be useful in connecting the first two, also in order to compute or estimate invariants.

On the other hand, the analysis carried out also suggests several possible developments, which could help to complete the picture of the existing relationships among the above theories. Our hope is that a unifying vision can offer deep and unexpected insights, allowing to improve the understanding of the topic.

As regards Section 3.1, an interesting development would be to obtain an algorithmic procedure to pass from Kirby diagrams to gems in the generalized case of diagrams representing also non-orientable 1-handles (according to [19]). If the resulting gems admitted gem-induced trisections (as happens in the orientable setting: see Theorem 17), in virtue of the non-orientable version of Laudenbach-Poenaru's result due to [31], an estimation of the trisection genus for all closed 4-manifolds would be

obtained, via gems.

Another possible improvement would be to study how to obtain a gem of a closed 4-manifold, starting from a gem of the compact one consisting only of handles up to order two, even if no ρ_3 - or ρ_4 -pair appears in the latter (as assumed in Proposition 9). The problem is obviously a difficult one, since it involves the combinatorial recognition of $\#_m(\mathbb{S}^1 \times \mathbb{S}^2)$ ($m > 0$) in 3-dimensional topology, but in specific situations it could possibly be faced, for example by detecting sequences of combinatorial moves yielding the desired ρ_3 -pairs.

For example, the gem depicted in Figure 22 (representing the orientable genus one 4-dimensional handlebody) contains no ρ_3 -pairs in its $\hat{4}$ -residue; however, by a sequence of combinatorial moves not affecting the represented 4-manifold (whose result is the “cyclic” exchanging of the end-points of three 1-colored edges), a ρ_3 -pair of color 1 appears in the $\hat{4}$ -residue, which is also a ρ_3 -pair in the 5-colored graph: see Figure 23, where the edges cyclically exchanged are highlighted in yellow, while the ρ_3 -pair is highlighted in blue. The ρ_3 -pair switching yields the 5-colored graph of Figure 24, which represents the 4-sphere; since a sphere-bundle summand is “lost” in the switching (according to Proposition 9(ii)), it is confirmed that the associated closed 4-manifold \bar{M} is $\mathbb{S}^1 \times \mathbb{S}^3$.

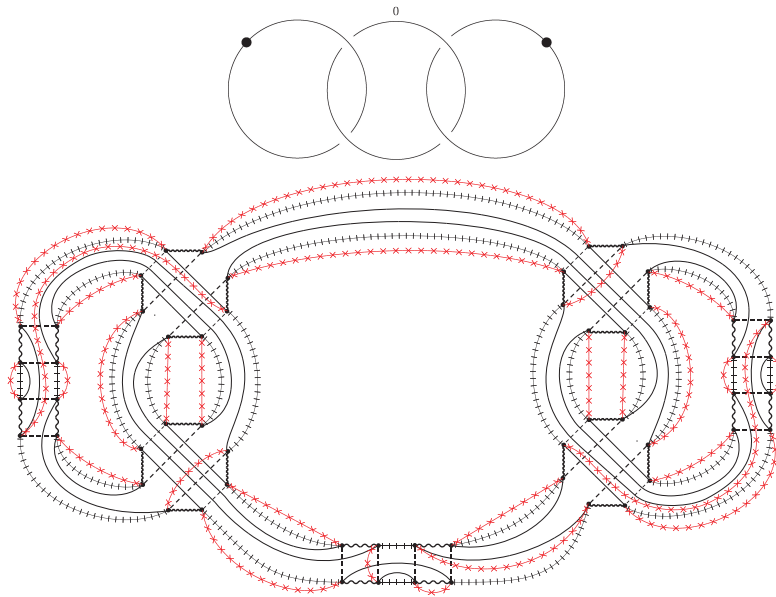


Figure 22: A Kirby diagram (L, d) (with two dotted components) and the associated 5-colored graph representing \mathbb{Y}_1^4

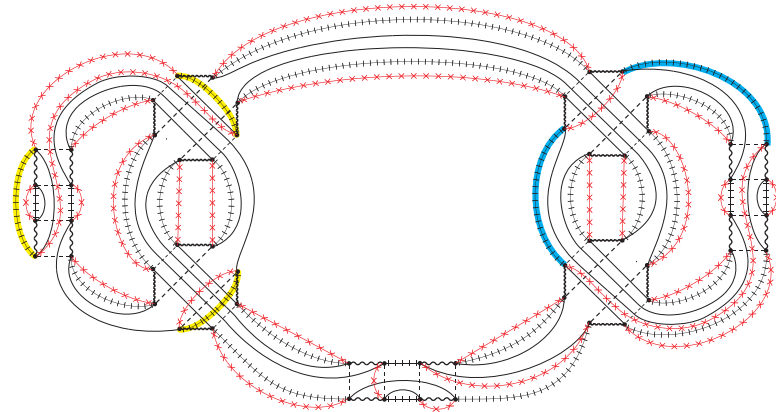


Figure 23: Another 5-colored graph (with a ρ_3 -pair) representing \mathbb{Y}_1^4

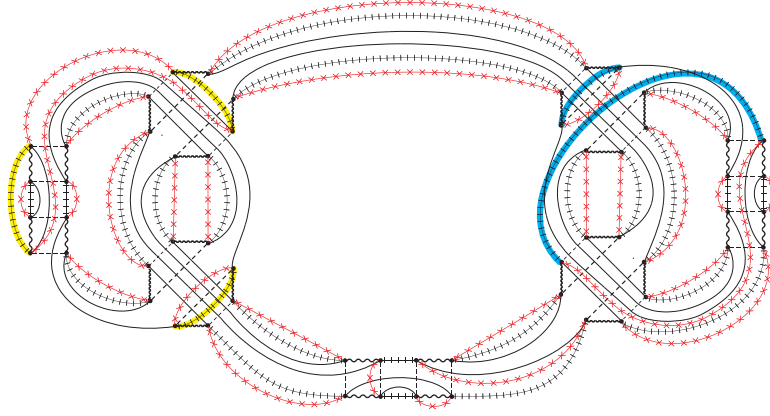


Figure 24: A 5-colored graph representing N^4 ($N^4 \cong \mathbb{S}^4$), so that $\bar{M} = (\mathbb{S}^1 \times \mathbb{S}^3) \# N^4$

With respect to Section 3.2, a fundamental problem involves the possible characterization of classes of gems so that the arising trisections (either directly, as gem-induced trisections, or indirectly, via the approach described in Section 3.2.2) realize the trisection genus of the represented 4-manifolds.

In [10, Section 6], a detailed analysis has already been performed in the case of 4-manifolds (with empty or connected boundary) admitting a gem-induced trisection $\mathcal{T}(\Gamma, \varepsilon)$ so that Γ is *weak semi-simple*¹³ with respect to the cyclic permutation ε of the color set. As a consequence, a large class of closed simply-connected 4-manifolds - comprehending all standard ones - has been identified for which the trisection genus equals the second Betti number and also coincides with half the regular genus, and an even larger class of such manifolds, for which the trisection genus equals the second Betti number¹⁴:

Proposition 26 ([10])

$$g_T(M) = \beta_2(M)$$

for each closed (simply-connected) 4-manifold M which admits a 5-colored graph $\Gamma \in G_s^{(4)}$ representing M with $g_{\varepsilon_0, \varepsilon_2, \varepsilon_4} = 1$ and $g_{\varepsilon_1, \varepsilon_3, \varepsilon_4} = 1$ (ε being a cyclic permutation of Δ_4), so that $\mathcal{T}(\Gamma, \varepsilon)$ is a gem-induced trisection.

In particular:

$$g_T(M) = \beta_2(M) = \frac{1}{2} \mathcal{G}(M)$$

for each closed (simply-connected) 4-manifold M admitting a crystallization Γ with $g_{\varepsilon_i, \varepsilon_{i+2}, \varepsilon_{i+4}} = 1 \ \forall i \in \Delta_4$ (ε being a cyclic permutation of Δ_4)¹⁵ and such that $\mathcal{T}(\Gamma, \varepsilon)$ is a gem-induced trisection.

It would be very interesting to characterize topologically 4-manifolds admitting gems which satisfy the hypotheses of the above statement, or at least to find classes satisfying them.

On the other hand, it would also be interesting to investigate conditions on the gems of a compact 4-manifold, so that the lower bound of Theorem 13 for the trisection genus of its associated closed 4-manifold is sharp.

Finally, we point out that some of the procedures described in Section 3.2 could be performed by suitable automatic implementations. In particular:

- Starting from a given gem (for example, by using its alphanumerical *code*: see [17]), it is possible to determine algorithmically the best choice of edges to use for stabilizations, so as to minimize

¹³A 5-colored graph $\Gamma \in G_s^{(4)}$, representing a compact 4-manifold M with empty or connected boundary, is said to be *weak semi-simple* with respect to a cyclic permutation ε of Δ_4 if $g_{\varepsilon_i, \varepsilon_{i+2}, \varepsilon_{i+4}} = 1 + m \ \forall i \in \{0, 2, 4\}$ and $g_{\varepsilon_i, \varepsilon_{i+2}, \varepsilon_{i+4}} = 1 + m' \ \forall i \in \{1, 3\}$ where $rk(\pi_1(M)) = m \geq 0$ and $rk(\pi_1(\widehat{M})) = m' \geq 0$.

¹⁴Note that for both classes the involved minimal trisections are *efficient*, according to [24].

¹⁵This condition is usually referred to by saying that Γ is *weak simple* with respect to ε .

the genus of the arising trisection, and hence get a better estimation of the trisection genus of the associated closed 4-manifold.

- Starting from a given gem, it is obviously possible to check in an automatic way whether condition (*) of Proposition 11 is satisfied; if so, it should not be difficult to detect algorithmically the bicolored cycles yielding a trisection diagram of the associated gem-induced trisection.

Acknowledgements: This work was supported by GNSAGA of INDAM and by the University of Modena and Reggio Emilia, project: “*Discrete Methods in Combinatorial Geometry and Geometric Topology*”.

References

- [1] P. Bandieri, C. Gagliardi: *Rigid gems in dimension n* , Bol. Soc. Mat. Mex. **18**(3), 55-67 (2012).
- [2] M. Bell, J. Hass, J. H. Rubinstein, S. Tillmann: *Computing trisections of 4-manifolds*, Proc. Nat. Acad. Sci. USA **115**(43), 10901-10907 (2018).
- [3] R.A. Burke: *Practical Software for Triangulating and Simplifying 4-Manifolds*, in: 40th International Symposium on Computational Geometry (SoCG 2024), Leibniz International Proceedings in Informatics (LIPIcs), **293**, 29:1-29:23.
- [4] R.A. Burke, B. Burton, J. Spreer: *Small Triangulations of 4-Manifolds: Introducing the 4-Manifold Census*, preprint. DOI: 10.48550/arXiv.2412.04768
- [5] B.A. Burton, R. Budney, W. Pettersson, et al.: *Regina: Software for low-dimensional topology*, <http://regina-normal.github.io/>, 1999–2023.
- [6] M. R. Casali, *From framed links to crystallizations of bounded 4-manifolds*, J. Knot Theory Ramifications **9** (4), 443-458 (2000).
- [7] M. R. Casali, P. Cristofori: *Cataloguing PL 4-manifolds by gem-complexity*, Electron. J. Combin. **22**(4), # P4.25 (2015).
- [8] M. R. Casali, P. Cristofori: *Kirby diagrams and 5-colored graphs representing compact 4-manifolds*, Rev. Mat. Complut. **36**, 899-931 (2023).
- [9] M. R. Casali, P. Cristofori: *Classifying compact 4-manifolds via generalized regular genus and G -degree*, Ann. Inst. Henri Poincaré Comb. Phys. Interact. **10**(1), 121-158 (2023).
- [10] M. R. Casali, P. Cristofori: *Gem-induced trisections of compact PL 4-manifolds*, Forum Math. **36**(1), 87-109 (2024).
- [11] M. R. Casali, P. Cristofori: *Trisections of PL 4-manifolds arising from colored triangulations*, Mediterr. J. Math. **22**, 27 (2025). <https://doi.org/10.1007/s00009-024-02790-2>
- [12] M. R. Casali, P. Cristofori: *Estimating trisection genus via gem theory*, preprint (2024).
- [13] M. R. Casali, P. Cristofori, C. Gagliardi: *Crystallizations of compact 4-manifolds minimizing combinatorially defined PL-invariants*, Rend. Istit. Mat. Univ. Trieste **52**, 431-458 (2020).
- [14] M. R. Casali, P. Cristofori, L. Grasselli: *G -degree for singular manifolds*, RACSAM **112**(3), 693-704 (2018).
- [15] M. R. Casali, P. Cristofori, S. Dartois, L. Grasselli: *Topology in colored tensor models via crystallization theory*, J. Geom. Phys. **129**, 142-167 (2018).
- [16] M. R. Casali, P. Cristofori, C. Gagliardi: *Classifying PL 4-manifolds via crystallizations: results and open problems*, in: “*Mathematical Tribute to Professor José María Montesinos Amilibia*”, Universidad Complutense Madrid (2016). <https://www.mat.ucm.es/josefer/otros/homenaje-montesinos.pdf>

- [17] M. R. Casali, C. Gagliardi: *A code for m -bipartite edge-coloured graphs*, Rend. Istit. Mat. Univ. Trieste **32**, 55-76 (2001).
- [18] N. A. Castro, D. T. Gay, J. Pinzon-Caicedo: *Trisections of 4-manifolds with boundary*, Proc. Nat. Acad. Sci. USA **115**(43), 10861-10868 (2018).
- [19] E.C. de Sá: *A link calculus for 4-manifolds*. In: Fenn, R. (eds), *Topology of Low-Dimensional Manifolds*, Lecture Notes in Mathematics **722**, Springer (1979).
- [20] M. Ferri, C. Gagliardi, L. Grasselli: *A graph-theoretical representation of PL-manifolds. A survey on crystallizations*, Aequationes Math. **31**, 121-141 (1986).
- [21] C. Gagliardi, G. Volzone: *Handles in Graphs and Sphere Bundles over S^1* , Europ. J. Combinatorics **8**, 151-158 (1987).
- [22] D. Gay, R. Kirby: *Trisecting 4-manifolds*, Geom. Topol. **20**, 3097-3132 (2016).
- [23] R.E. Gompf, A.I. Stipsicz: *4-manifolds and Kirby calculus*. American Mathematical Society, **20**, (1999).
- [24] P. Lambert-Cole, J. Meier: *Bridge trisections in rational surfaces*, Journal of Topology and Analysis **14**(3), 655-708 (2022).
- [25] F. Laudenbach, V. Poenaru: *A note on 4-dimensional handlebodies*, Bull. Soc. Math. France **100**, 337-344 (1972).
- [26] S. Lins: *Gems, computers and attractors for 3-manifolds*. Knots and Everything, no. 5. World Scientific, River Edge, NJ, 1995.
- [27] R. Mandelbaum: *Four-dimensional topology: an introduction*, Bull. Amer. Math. Soc. **2**, 1-159 (1980).
- [28] R. Martini, R. Toriumi: *Trisections in colored tensor models*, Ann. Inst. Henri Poincaré Comb. Phys. Interact. **11**(3), 453-502 (2024).
- [29] J. Meier: *Trisections and spun 4-manifolds*, Math. Res. Lett. **25**(5), 1497-1524 (2018).
- [30] J. Meier, T. Schirmer, A. Zupan: *Classification of trisections and the Generalized Property R Conjecture*, Proc. Amer. Math. Soc. **144**(11), 4983-4997 (2016).
- [31] M. Miller, P. Naylor: *Trisections of non-orientable 4-manifolds*, Michigan Math. J. **74**(2), 403-447 (2024).
- [32] J. M. Montesinos: *Heegaard diagrams for closed 4-manifolds*, in: "Geometric Topology", Academic Press (1979).
- [33] J. H. Rubinstein, S. Tillmann: *Multisections of piecewise linear manifolds*, Indiana Univ. Math. J. **69**(6), 2209-2239 (2020).
- [34] J. Spreer, S. Tillmann: *Determining the Trisection Genus of Orientable and Non-Orientable PL 4-Manifolds through Triangulations*, Exp. Math. **31**(3), 897-907 (2022).
- [35] B. Trace: *On attaching 3-handles to a 1-connected 4-manifold*, Pacific Journal of Mathematics, **99**(1), 175-181 (1982).